1-1-2015

Programmable Dna Delivery To Cells Using Bioreducible Layer-By-Layer (lbl) Polyelectrolyte Thin Films

Maria Muniz
Wayne State University,

PROGRAMMABLE DNA DELIVERY TO CELLS USING BIOREDUCIBLE LAYER-BY-LAYER (LBL) POLYELECTROLYTE THIN FILMS

by

MARIA MUÑIZ

THESIS

Submitted to the Graduate School

of Wayne State University,

Detroit, Michigan

in partial fulfillment of the requirements

for the degree of

MASTER OF SCIENCE

2015

MAJOR: BIOMEDICAL ENGINEERING

Approved By:

_____

Advisor Date

ACKNOWLEDGEMENTS

I would like to thank my advisor, Dr. Guangzhao Mao and co-advisor Dr. Weiping Ren, whose wisdom, guidance, and patience made this work possible. Thank you for introducing me to the fascinating research at the intersection of biomedical engineering and chemical engineering. This has been a wonderful opportunity and I thank you for your support.

I would like to thank my committee members, Dr. Howard Matthew and Dr. Harini Sundararaghavan for their support and suggestions.

I would like to thank all of the research groups I have collaborated with throughout my thesis research, including Dr. Wei-Zen Wei, Dr. Haipeng Liu, and Dr. Zhiqiang Cao. Additionally, lab members from the Cao, Da Rocha, Matthew, Ren, and Wei labs. I sincerely appreciate the time you took to assist me and expertise you all provided. A special thanks is reserved for Heather Gibson, whose patience and kindness will not soon be forgotten.

I would like to thank the members of my own lab, especially Lingxiao Xie, whose reliability and hard work were invaluable throughout my time at Wayne State. I am grateful for all you have taught me.

Last I would like to acknowledge my family, and my significant other, Collin Johnson, for their unconditional support.

TABLE OF CONTENTS

LIST OF FIGURES

CHAPTER 1 INTRODUCTION

Drug and gene delivery: background and biomedical application of thin film technology

Thin films are an important technology in the field of biomedical engineering. The concept of these film systems are extraordinarily simple: just repeated layers of reagents on a substrate of interest. The substrate can then be implanted into the body, either short or long term, and through chemical or biological interactions, the films degrade, releasing their cargo. These thin films can be thought of as tiny reservoirs that can be implanted into the body, allowing incorporation of therapeutic agents in a controlled, precise manner.

Therapeutics include delivery of genes, drugs, biological signaling proteins, and antibiotics among others. Depending on the composition and structure of these thin films, they can provide specific release profiles that can lead to systemic therapeutic integration, but importantly, and arguably more useful, they can provide targeted release to a local environment, thus sparing the body from the effects of unnecessary and unneeded chemicals, while simultaneously decreasing the amount of material needed in order to provide therapy. Instead of releasing an agent in to the system where it is subject to dilution, filtration and removal, degradation, and inactivation, a small amount of very potent agent can be used and delivered directly to the area of interest, bypassing all of the aforementioned ill effects. In contrast to intravenous administration of agents, the wait for the agent to be circulated throughout the bloodstream before being delivered to the area is vastly decreased. In contrast to local injections or therapies, the agents can be modified to release only when chemically or biologically signaled, and the timing of release can also be tailored to specific therapeutic needs.

Non-viral polyelectrolyte thin film technology has vast applications in a number of different areas, including tissue engineering (delivery of growth factors, genes, and multi-component biological signaling systems), trans-dermal and implantable therapies (delivery of drugs, antibiotics, and other therapeutics), and vaccines (delivery of adjuvant agents and eliciting immune response). One promising example for the therapeutic application includes cancer treatment with polyelectrolyte multilayered implants containing hazardous, known as “low therapeutic index”, drugs. Because of their high risk of toxicity, the implant could be situated near or in direct contact with the tumor, ensuring long-term sustained release of the drug, but only to the affected area [1].

Another section of biomedical engineering that benefits from LbL technology includes tissue

engineering and other biological signaling systems that work synergistically with the body in order to enhance or promote growth. Applications notably include bone tissue engineering to mend defects after trauma, or aid in bone integration after implants. The latter is a large area of interest, considering the growing aging population and subsequently both the large number of orthopedic implants and large number of losses from complications with these implants.

In the United States alone, the cost of complications from just hip implants are on the scale of $1 billion per year [2]. Knee replacements also make up a large number of surgical procedures performed each year, with knee replacements in the United States numbering upwards of 700,000 in 2011 [3]. Together, these two orthopedic implants made up almost 8% of all operating room procedures in the United States in 2011 [3]. The incidence of knee and hip replacements, respectively is projected to rise to over 3 million procedures per year and over 500,000 procedures per year by the next 15 years [4], showing the burgeoning demand for improved technology in this field. One of the major setbacks currently with orthopedic implantables is lack, or delayed failure, of bone and tissue integration in and around the implant, leading to loosening and many times, revision of the implants and additional surgery. Shah et. al write "Approximately 10% of total hip prostheses (THP) are revised within 10 years after the procedure due to loosening of the implant [5], almost entirely because of the failure of fixation in cases of aseptic loosening [6]. In order to engineer a successful implant, it is necessary to address the bone as a highly vascularized tissue where a multistep process involving migration, proliferation, differentiation, and activation of several cell types is necessary for integrating the implant with the bone tissue [7, 8]".

Using LbL technology, implant surfaces can be optimized to create the ideal environment to facilitate vascularization, bone generation and integration, and antibiotic protection. Interestingly, the layer-by-layer design is especially tailored to the application of bone regeneration because it requires a number of different, sequential, cytokines in order to be successful. Having the ability to add all of the bone morphogenic proteins, transforming growth factors, and fibroblast growth factors that the osteogenesis process needs into the films, and having the added benefit of being able to adjust their release times and duration by adjusting the film architecture, using LbL technology to coat orthopedic implants could lead to better success rates for these invasive surgeries [9].

An additional application where non-viral LbL polymeric thin film technology is of great potential benefit is in the area of therapeutics, wherein drugs, antibiotics, genes, or other treatments are delivered. With mild synthesis conditions that would otherwise damage or inactivate sensitive biological drugs in harsher manufacturing techniques, this technology shows great promise to deliver a variety of biologicals including drugs, therapeutic proteins, synthetic or natural polyelectrolytes,

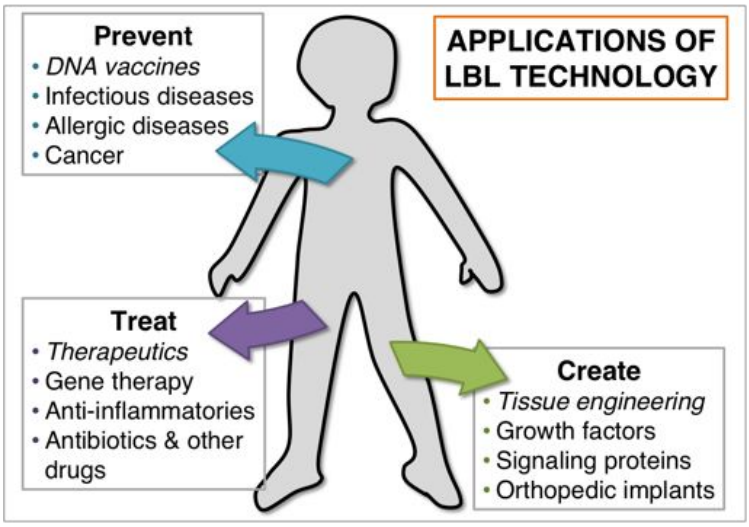

Figure 0.1: Biomedical applications of LbL technology, categorized

and other small molecules all while retaining functionality [10, 11]. There is particular benefit in the areas of implants and devices, most notably in the orthopedic and cardiovascular areas [12], where treatment of secondary complications such as clotting and infection are of critical importance to both implant success and patient health. In contrast to other delivery methods which may not be able to administer high enough doses of the active material to treat existing infection, LbL technology allows for high loading capacity of the biological agents, which in turn allows for high doses of active material to be delivered successfully to the treatment area [10].

One practical example of the utility of the LbL technology is developing an anti-inflammatory biomaterial coating. Anti-inflammatory coatings are of great value to the entire field of biomedical implants, as chronic inflammation and other complications can often undermine the benefit, limit the use, and even result in removal of the implants [11]. To treat the foreign body response due to implant trauma, systemic treatment with steroidal and non-steroidal drugs can be administered, but comes with its own risks and major side effects [11]. This further underscores the utility of LbL films as a local, direct delivery system. In a study examining the functionality of an anti-inflammatory biomaterial coatings, a signal protein was embedded within a polyelectrolyte multilayer film. It was found through cellular interaction experiments that, in comparison to other methods of attaching the anti-inflammatory agent to an implant, the LbL technology allows for retention of the agent's active biological properties [11]. Also highlighted in this study is one of the major advantages of the LbL system, which is the ability to provide long lasting sequential versus bulk release by altering the film architecture. This is particularly important for anti-inflammatory and antibiotic film applications which often require sustained drug delivery in order to be successful.

Although LbL technology is particularly useful for long term and temporally sensitive applications, a separate study examined the use of LbL films for anti-inflammatory response, aimed towards more short-term use. The study utilized LbL films to inhibit pro-inflammatory cytokines such as TNF-α that can lead to compound complications and septic shock. It was found that a pro-inflammatory factor could be prevented at the source by inhibiting their production by macrophages [13]. It was speculated that this LbL film could be incorporated onto surgical situations and developments of "microbial remediation technologies" wherein infection and shock could be avoided by preventing catastrophic inflammation cascades [13].

With modern advancements in both the understanding and technology in the fields of medicine and molecular biology, comes the opportunity for the development of therapies on the genetic level[14]. Many genes have been implicated in diseases, syndromes, and disorders, through the completion of the human genome project [15]. Some noted applications of gene therapy include sickle cell disease [16], Parkinson's disease [17], Duchenne muscular dystrophy [18], cystic fibrosis [19], and haemophilia B [20]. There are many studies developing gene delivery therapies, and many of these strategies show potential to be translated into polymeric thin film technology. The ability to control the release timing of LbL films make them a perfect candidate for gene delivery systems, which, for many chronic diseases, metabolic defects, and genetic issues require long-term administration [1, 15]. The advantage of LbL technology for gene therapy is the ability to ensure sequential release of different genes and components at specific times, due to the component flexibility of the layered architecture.

In the field of cancer therapy, methods of using LbL technology to prevent bone metastasis are being investigated. Bisphosphonate drugs are a class of anti-tumor chemicals used for treatment of bone metastases, or primary tumor that spreads to the bones as a secondary tumor. This class of drugs works to combat the unbalanced remodeling of bone caused by the bone metastasis and decreases pain, fractures, and bone resorption [21]. By using a bisphosphonate drug as an active layer on a multilayered polymer-based bone implant coating, researchers found promising results that suggested efficacy of the polymer/drug complexes from the films to enhance cellular uptake of the drugs and prevent bone metastasis in vitro and in animals [22]. It is anticipated that coating implants with these drug-loaded polymeric films could decrease the amount of drug necessary for successful therapy, thus minimizing adverse side effects, while simultaneously reducing waste of therapeutics [22].

While we have explored the creation and treatment aspects of gene and drug delivery through LbL technology, another application with vast public health implications is the concept of LbL-based

vaccines. Vaccines, and DNA vaccines in particular, are a concept that are already being explored in the field biomedical engineering, and uses include "prophylactic vaccines, to immunotherapy for infectious diseases, cancer, and autoimmune and allergic diseases" [23].

The method for DNA vaccines employ a plasmid that encodes for the disease antigen. This plasmid undergoes cellular uptake and gene expression and the antigen is presented to the appropriate immune components and an immune response is elicited. In addition to the antigen encoded in the plasmid, the plasmid itself can act as an adjuvant as well, due to its non-mammalian nature and different methylation character [24, 25, 26]. Other gene therapy/vaccines are highly complex, sometimes involving extraction and implantation of cells, and also high risk, altering pathogenic or immunogenic viruses and bacteria [23]. Encoding for an antigen rather than using the actual virus, (whether live or attenuated), is considered safer for certain high-risk diseases such as HIV [27].

In comparing different vaccination methods, it has recently been investigated that a specific response from the CD8+ cytolytic T, or, CTL cells, was of particular importance to the success of generating a complete, more robust immune response [23]. While it seems recombinant protein or inactivated virus vaccines lack the proper cellular trafficking in order to elicit a full immune reaction including CTL response [28], LbL technology could be tailored to create a polymeric gene delivery system that targets this important immune response. Recently, Shah et al. wrote "In addition to the potential safety benefits, such non-viral systems offer greater structural and chemical versatility for manipulating physicochemical properties, vector stability upon storage and reconstitution, and a larger gene capacity compared to their viral counterparts" [8].

The vast applications for LbL polymeric thin film technology have been outlined. The implications for growing this technology are great; although transfection is the greatest limiting factor for LbL drug- and gene- delivery, the benefits are vast. The main methods of gene delivery can be divided into two categories: viral and non-viral. Although viral vectors have been shown to be efficient gene delivery agents, synthetic, polymeric non-viral vectors show promise to transfer genes, drugs, and other small molecules in a safer manner. The category of non-viral vectors that will be featured here is the bioreducible, controlled release, polyelectrolyte LbL thin film system. These particular film delivery systems have enormous potential for use in the biomedical sciences field because of their high level of chemical customization and ability to be adapted to a variety of therapeutic applications, their stability in physiological environments [1], safety [8], and ability to conform to a wide variety of complex implant geometries [12].

Nearly every aspect of the LbL system can be customized to meet the needs of the application. Starting with the polymeric constituents, flexibility in polymer chemistry can be taken advantage

of in order to synthesize thin film components that maintain biocompatibility while maintaining transfection, or ability to delivery agents effectively [15]. Load capacity can be easily adjusted incrementally by increasing or decreasing quantity of layers. The LbL film components and architecture can be further fine-tuned in order to accommodate multiple genes/agents if extended exposure/therapy times are required. Additionally, polymeric barrier layers can be introduced into the architecture, further tuning the release characteristics of these films, from burst release, to continuous release and everything in between.

Manufacturing of LbL materials is straightforward and safe. Dip coating of polyelectrolyte materials for LbL thin films takes place at room temperature, in stable aqueous solutions that don't require special handling or environment. Harsh solvents are not required, the equipment is minimal, and the process is simple. Being able to perform the thin film dip-coating at room temperature also allows for a variety of fragile biologic materials, such as proteins, to remain in their active form during the process [12]. Another quality of LbL films which makes the technology easy to implement is that the characterization methods used for evaluating these coatings are well established characterization methods [1], such as such as ellipsometry and AFM used our recent studies.

LbL films can be coated on myriad surfaces, from stents, sutures, pacemakers, orthopedic, cardiac, and other implantable devices as well as skin penetrating devices [10]. The dip coating process is simple and extremely flexible. These nanometer-scale thin films can easily be coated onto implantable surfaces or devices of different shape, size, or composition. The aqueous dipping solution can be contained in any container imaginable to accommodate whatever the geometry of the implant or device.

Additionally, coating implants with drugs and other therapeutic agents minimizes the distance between active ingredient and target area. This is a key feature that adds to the safety and utility of the LbL system. It is anticipated that this would be of special utility for applications where systemic exposure needs to be minimized due to side effects, and also in applications where the high doses needed for treatment are difficult to obtain through systemic administration routes. In a recent commentary, de Villiers, et al. write: "LbL self-assembly systems therefore proved a very robust platform to create novel, hybrid or stabilized drug deliver systems for a myriad drugs and genes can be employed on various nano- to macroscopically-sized systems. Due to its technological ease and cost of preparation, avoidance of hazardous preparative chemicals, independence of precise stoichiometry, facilitation of controlled, triggered and target release, the technique should see significant growth in future as a leading drug delivery technology" [1].

Layer by layer polymeric thin film transfection: mechanisms, hurdles, and our approach

Unlike viruses, which have adapted methods to circumvent the cells' biological defenses, polymeric delivery vectors must be engineered precisely in order to successfully transfect a cell. The cellular defense mechanisms are many and complex. "For efficient nucleic acid delivery, polymeric carriers have to cope with apparently contradictory demands: to stabilize the nucleic acid against degradation, but release it at its biological site of action; to shield the polyplex during circulation in the blood stream, but to de-shield it upon cell entry; and to leave the cell membranes intact, but to rapidly destabilize the endosomal membrane [29]." For transfection to occur in our delivery system, the LbL film must have the correct combination of components in order to positively interact with the cellular surface and begin the pathway to endocytosis. At the same time, the polyelectrolytes in the film must be such that the condense the DNA present in the film to a small enough polyplex particle that it favors endocytosis. The delivery system must perform all of these duties while still remaining non-toxic and biocompatible (figure **??**). There are a number of common DNA different delivery approaches employed for polymeric thin film systems including pH or ionic destabilization, receptor-ligand disassembly, DNA release triggered by energetic stimuli, or using enzymatically cleavable polyelectrolytes, which is the method we use[30]. The polymers we choose for our LbL films are polyamidoamine (PAA) polycations that feature disulfide bonds. The presence of this bond allows interaction with the cell surface and reduction of the polymer 0.3. The polycationic material is able to electrostatically bond to and condense the DNA and a polyplex is formed. The polyplex is a small globular complex (few tens to several hundred nanometers in diameter) with supercoiled DNA at its core with a positively charged polyelectrolyte shell, enabling protection of the genes and mediation of cellular entry [15]. This polyplex must then enter the cell using one of many endocytic pathways **??**. As seen in figure 0.2, the polyplex must then travel through the cell, overcoming barriers such as degradation and entering the endolysosomal or exocytosis pathways. Finally, the polyplex must unpack its DNA cargo so it can pass through the nuclear envelope where it can finally be incorporated into cell processes and the gene can be expressed. It is important to point out that for some steps, many different pathways exist and for others, mechanisms of action are poorly understood. This elaborate process showcases the complexity of the non-viral gene delivery problem, and underscores the quantity of considerations for designing these polymeric drug carrier systems.

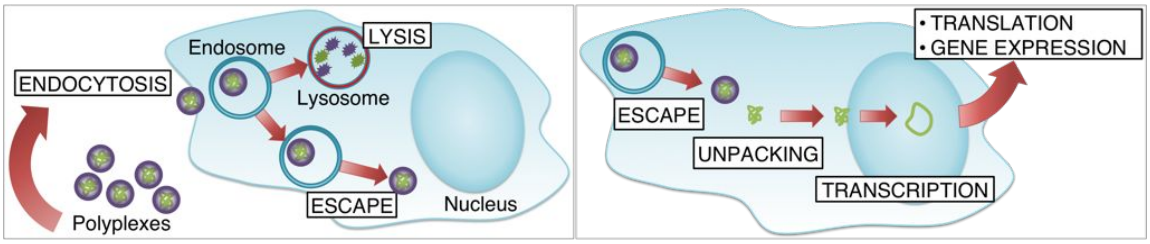

Figure 0.2: An outline of polyplex cellular entry. Many processes (including specific endocytosis pathway), have been simplified in order to convey the process as a whole in a more clear manner. Left: After polyplex formation, the cell can endocytose the complex where it enters an endosome or escapes lysis and enters the cytoplasm. Right: Once the polyplex enters the cytoplasm, the polycathodic shell of the polyplex must release the DNA. Where this unpacking occurs is not certain. After entering the nucleus, the DNA is transcribed and finally, gene expression occurs, in our case signified by producing green fluorescent protein.

Extracellular issues

One of the first things to consider for the LbL system is keeping the DNA intact throughout its entire journey to the nucleus. The polycation in our system is responsible for condensing and thus ensuring protection of the DNA. In a realistic implant scenario, naked DNA located in the extracellular surroundings can garner non-specific interactions due to the many proteins and other positively-charged molecules that are present in the blood and bodily fluids, even in the artificial in vitro environment where media and serum are in contact with the system. These non-specific interactions can not only lead to aggregation but also detection by the immune cells, both leading to prevention of the DNA being successfully delivered to its target cell. There are a number of important considerations when choosing a polycation to condense the DNA of the LbL system, and recent studies show at least some factors that have been identified. "... charge density, rigidity, basicity, buffer capacity, hydrophilicity/hydrophobicity, type and number of amino groups, backbone degradability and specific interaction groups are recognized to influence gene delivery properties such as DNA binding capability, colloidal stability, endosomal escape (buffer capacity), vector unpacking and cytotoxicity. Therefore, optimal combination of various functionalities is necessary to obtain multifunctional polymeric vectors that are capable to overcome the multiple gene delivery barriers and yield high transfection efficiencies [31]."

As mentioned previously, the class of polyelectrolytes used in our system are the bioreducible disulfide bond containing-polyamidoamines (going forward, these will simply be referred to as PAAs). These polymers are especially suited for gene delivery as they are stable in the extracellular environment, but they undergo rapid degradation in the intracellular environment because of high concentrations of reductase enzymes that degrade these bonds [32]. Studies suggest that disulfide bond reduction begins with the interaction of the cell with the film surface (figure 0.3)

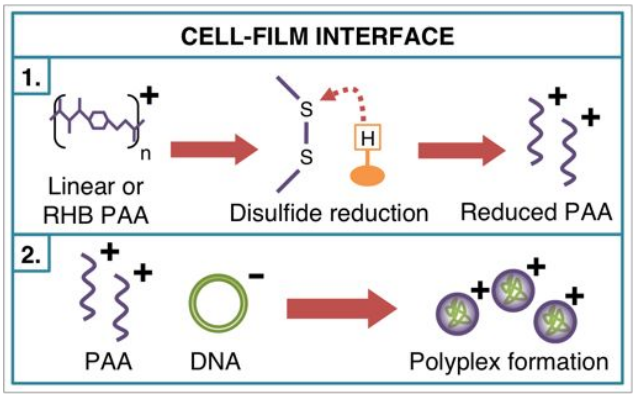

Figure 0.3: Simplification of the interaction at the extracellular surface of the cell in contact with the bioreducible LbL thin films. The disulfide bonds present in the polyamidoamine polycathode undergo a disulfide reduction reaction with various surface proteins.

and continues through endocytosis [33]. Disulfide bond-containing PAAs used in our films display a number of features that have been shown to lead to increased transfection efficiency. The disulfide bonds in the backbone enables fast intracellular polymer fragmentation which should lead to decreased cytotoxicity and also facilitates gene unpacking [31]. Transfection is facilitated by more hydrophobic side groups (by increasing polyplex interaction with the cell membrane [31], having higher primary amine content [34] or higher charge density [32] (by increasing condensation and forming smaller polyplexes with high surface charge). Poly 5-amino-1-pentanol (APOL) in particular was shown to induce a high transfection efficiency because of its good DNA binding ability and its buffer capacity [31], and was used in our later experiments to much success.

Design elements employed to prevent aggregation and/or clearance by phagocytes of polymer fragments and polyplexes in the in vivo setting will not be discussed in detail, as our LbL drug delivery system is still in the in vitro testing stage. However, considerations of the system include protection from serum protein adsorption and immune system attack and clearance and ensuring a high polymer/DNA charge ratio (comparing the negative DNA backbone phosphates to the positive polycation amines) to ensure rapid unobstructed uptake by the targeted cell(s). Once the DNA is condensed safely inside of the positively-charged polycation structure, polyplexes must successfully make contact with the negatively charged cell surface and undergo endocytosis by one or more of a variety of different pathways.

Endocytosis

One of the benefits of using synthesized polymers in these drug/DNA delivery systems is that the chemistry of the polymer can be modified quite easily in order to better guarantee entry into the cell via endocytosis. Although we do not explore in vivo testing here, designing of our polymeric carriers takes into account as many in vivo issues as possible. Unfortunately, current understanding of the uptake and trafficking mechanisms of these polyplexes only offers a conjecture into their endocytic pathway due to the widespread variation in results between cell type, polymer type, cell cycle, polyplex size, and cell polarization state, among other variables [35, 34]

There are a number of different endocytosis pathways, including those shown in figure **??**, spanning from receptor-mediated endocytosis, phagocytosis, non-specific ionic interactions with proteoglycans, non-specific lipophilic interactions with phospholipid components, and cell penetrating peptide (CPP)-mediated uptake [14]. These pathways can be divided into targeted uptake (clathrin dependent) and non specific uptake (clathrin independent) categories. Clathrin dependent pathways include receptor-mediated endocytosis and phagocytosis. Studies suggest that endocytic pathway of particles is size dependent, and studies observed that particles around 50-200 nm use these clathrin dependent mechanisms [29]. Most polyplexes for drug delivery, including those that are generated at our LbL film-cell interface, are in this size range, and subsequently, it is suspected [34] that most polyplexes enter the cell via the clathrin-mediated endocytosis pathway.

Unfortunately, it has also been suggested that internalization via this specific pathway may lead to trafficking within the degradative, lysosomal pathway [36]. Lysosomes are loaded with degradative enzymes and are able to create a concentrated acidic environment that quickly disintegrates its contents. Thus, it is of particular interest to optimize the characteristics of our polyplexes in order to successfully escape the lysosome. PEI, the barrier layer contained in our Type B LbL films, is known to have special characteristics that make it much more likely to be successful in endolysosomal escape. Other, endocytic pathways include the clathrin independent pathways via caveolin-dependent or caveolin-independent methods (which don't necessarily sort contents into lysosomes), and it is noteworthy to mention that multiple endocytic methods may be active on any one cell [34]. If the polyplexes are able to evade both exocytosis and lysis, then they must escape the endosome and trafficking through the cytoplasm and toward the nucleus begins.

Endogenous issues and nuclear transport

The complicated travels of polyplexes are further compounded by studies that suggest specific internalization pathway has an effect on polyplexes intracellular processing and subsequently their transfection [35]. Indeed, internalization of the polyplex is only the first hurdle overcome in the complex transfection process. One study estimated that upwards of 95% of cell in culture will internalize the delivery vectors (polyplexes) as low as fewer than 50% may express the gene in the end [15]. It is therefore especially valuable to understand the movement of these polyplexes as they travel through the cell, and to optimize their features to encourage delivery to the nucleus. Unfortunately, the methods of polyplex escape, DNA unpacking, and delivery to the nucleus are all poorly understood mechanisms. Suh et al [37] used real-time particle tracking to quantify non-viral DNA nanocarrier movement inside the cell and found similarities between PEI/DNA nanocomplexes and DNA viruses found in nature. Mechanisms such as motor-driven cytoplasmic transport, active gene carrier transport, and microtubule involvement were shown, but it was noted that the success of these mechanisms is dependent on a wide variety of factors that need to be further identified and investigated.

One approach to enhance endosomal escape is to attach peptides to the polymers which would be pH triggered to disrupt the membrane when activated, thus freeing the polyplex [15]. There are a number of factors that influence the polyplex's ability to successfully escape the endosome. One of these is based on the so-called "proton-sponge hypothesis", depicted in figure**??**. PEI, as used in our Type B films, is a known proton-sponge polymer, but the proton-sponge capability is not limited to just PEI [34, 15]. Proton sponge polymers have substantial secondary and tertiary amines and "pKA values between physiological and lysosomal pH [15]." A polyplex (containing the proton-sponge polymer) can protonate after being internalized by the endosome, creating an influx of protons. The protons are balanced by counterions as the endosome attempts to regulate the pH. This extreme excess of ions inside of the endosome causes osmotic swelling, increased pressure, and ultimately, rupture [15]. Disulfide-containing polymers have also been associated with proton-sponge activity. One study tested a variety of disulfide-containing PAAs and found that nearly all exhibited excellent buffer capacity, which is an indicator of its ability to act as a proton sponge [32]. It is anticipated that the high buffer capacity, coupled with the presence of the reducible disulfide bond, could imply better success for endosomal escape [32] for DNA de-shielding after escape [15], and eventual success in gene transfection [33].

Since the cytoplasm is full of nucleases and a formidable environment for unprotected DNA,

it is most likely that the polyplex is transported through the cytosol and near the nucleus before unpacking the vulnerable DNA. One study showed, however, the presence of intact polyplexes in the nucleus, but also free DNA in the cytosol [29]. The mechanism in which the transport occurs is unfortunately unclear, but it is hypothesized that there is microtubule involvement. Active transport via microtubules is a method viral vectors use to locate near the nucleus, and could either bring the unprotected DNA or the complete polyplex containing the DNA towards the nucleus [37]. While it is understood that the likelihood of transfection is larger if the DNA is closer to the nucleus, it has also been shown in many studies that transfection is highly dependent on cell type, and most importantly, cell cycle [38, 39, 40]. One theory is that if polyplex uptake and endosomal escape occur just before mitosis, the mixing of cellular contents that occurs during the process would place some polyplexes near or in the nucleus [15]. In fact, it has been noted that nuclear entry occurs more frequently when the cell is undergoing mitosis [38], and noted an increase in transfection efficiency occurs in cells transfected "shortly before their next cell division (cells in late S/G2) [39]." Regardless of the exact mechanism that determines transfection, the characteristics of the polyplex indicate that it will enter the nucleus via a passive pathway, not involving any nuclear localization signals nor entry through the nuclear pore complex (NPC) [40].

The type of polymer involved also has strong influence over unpacking of the polyplex in the cytoplasm and successful transfection. Unfortunately, "...strong binding and efficient DNA condensation do not correlate directly with gene-delivery efficiency [15]." As outlined previously, the use of polymers with disulfide bonds increases a polyplex's ability to escape and unpack. Although our PAAs undergo bond breaking in order to form the initial polyplex structure before entry into the cell, it is noted that glutathione in the cytoplasm can reduce any remaining disulfide bonds in the polyplex that has escaped the endosome, leading to release of the DNA cargo inside of the cytosol [15, 32]. Type of amino group and the amino spacer length have both been found to affect transfection efficiency and also cytotoxicity [31]. There are a number of other characteristics that increase likelihood of polyplex unpacking, including using shorter, lower molecular weight polycations, by causing weaker binding to the DNA by reducing number of positive charges on the polycation, and using smaller DNA plasmids to facilitate movement [41, 15]. Although there is still much to be learned and understood about the mechanisms which lead to successful nuclear entry and transfection, our disulfide bond-containing PAAs are highly reducible, and our DNA plasmid is simple and small.

Our approach was to create a non-viral polyelectrolyte LbL thin film to deliver DNA to cells in a controlled, efficient, non-toxic manner. Our films utilize many house-synthesized polyelectrolytes

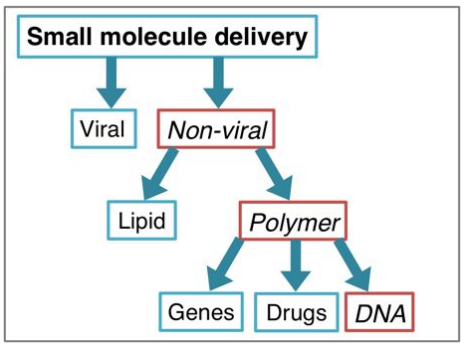

Figure 0.4: Non-viral gene delivery methods - the big picture, and where our technology fits in.

that we introduced one by one into the same (with some exceptions) bilayer film structure. Before performing in vitro experiments with 3 main cell types, we tested the polymer binding and transfection efficiency by running polyplex experiments. By combining polycationic material and DNA in a controlled manner, we were able to gain a better understanding of its condensation and transfection ability on cells in culture. We combined the different polycation choices with different enhancing materials embedded into the films, as well. We employ a number of biologic materials including hyaluronic acid, RGD peptide, fibronectin, and chitosan. As an additional layer of enhancement, we also tested changing different structural and mechanical properties of the films to see how this influenced the transfection. Finally, we systematically changed variables in the in vitro set up and environment in order to optimize cell health and transfection.

CHAPTER 2 MATERIALS AND METHODS

Experimental overview

In summary, polymers were tested using polyplex experiments first. Afterward, a set up for the film structure was determined. All of the reagents for the films were made. The films were then constructed using the dip coating method. Often, the build-up process was monitored using AFM. Cells were grown and a variety of cell conditions were tested, mostly cell seeding density. Before constructing a new LbL film for in vitro cell studies, proposed modifications to the polymer chemistry and film composition are tested by first using a polyplex testing method.

Using a polyplex before moving on to the more intensive biological studies prevents squandering time and materials. Our polyplex experiment spans 3 days if the cells have been maintained in culture, and uses micrograms of plasmid DNA. This is in contrast to even a single in vitro cell study which consumes milligrams of DNA and takes up to 2 weeks. A polyplex is formed by the electrostatic interactions of the DNA and an available polycation, causing condensation of DNA, with its negative phosphates inside of a polycation shell...entropically driven [42]. The process reduces the size of the DNA into a nano-scale structure that can more easily be endocytosed by cells to allow transfection. The clinical application of polyplexes is somewhat limited, yet they can be used as a a test for new combinations of polycations to be used in layer by layer film fabrication.

Cells

Cells used in all of the in vitro experiments were received in culture from collaborating Wayne State University laboratories. The MC3T3 preosteoblast cell line derived from newborn mouse calvaria and the mouse monocyte/macrophage cell line RAW were obtained from Dr. Weiping Ren. The HEK-293 cell line derived from fetal human embryonic kidney and the NIH/3T3 fibroblast cell line derived from embryonic mouse were both obtained from Dr. Weizen Wei. The cells were propagated using standard sterile culture techniques, and grown in under "normal" conditions at 5% CO_2, 37 ^{o}C, in a humidified incubator. Cell-appropriate media was obtained from Invitrogen and supplemented with 10% FBS (Fetal Bovine Serum-Advantage, Atlanta Biologicals) and 1% penicillin streptomycin (Invitrogen, 10,000 U/mL).

For the MC3T3 cells, α-MEM media (nucleosides, Life Technologies, Gibco), for the HEK-293 cells and NIH/3T3 cells, DMEM media (high glucose, pyruvate, Life Technologies, Gibco) was

used. Trypsin EDTA (0.25%, phenol red, Gibco) was used to dissociate cells when needed, and 1x phosphate-buffered saline (PBS) without calcium, magnesium, or phenol red (pH 7.4, Gibco) was used for washing and reconstituting reagents.

In order to prevent adhesion of cells to the underside of the glass substrate, 24-well standard tissue-culture treated plates (Sigma-Aldrich) were coated with poly(2-hydroxyethyl methacrylate) $(C_6H_{10}O_3)_n$, or, poly-HEMA. Briefly, poly-HEMA (Sigma-Aldrich, BioReagent powder) was dissolved, stirring constantly, at a concentration of 20 mg/mL in 95% ethanol under 40 ^{o}C, closed conditions to prevent evaporation. For a 24-well plate, ~100 µl was evenly distributed on the bottom of each cell well and allowed to dry overnight in a cell culture hood under sterile conditions. Afterwards, dried plates were either used immediately or sealed with Parafilm® and stored at room temperature for later use. By coating the multi-well plates with poly-HEMA prior to using, few, if any cells were able to attach to the bottom of the substrate in in vitro cell studies. This prevented cells from growing on multiple focal planes and obscuring microscopy results.

Plasmid DNA

Transformation

Plasmid DNA (pDNA) was generated for further amplification by selecting a single transformant obtained by chemical transformation of TOP10 chemically competent *E. coli*. Transformation of the *E. coli* bacteria is needed in order to further use it as a reporter, as it must uptake, through the cell membrane, the foreign DNA of interest and incorporate it into its own genome. In these experiments, the enhanced green fluorescent protein (EGFP) gene and the kanamycin resistance genes are the specific genes of interest, and the plasmid DNA used includes these genes in addition to other standard promoters, enhancers, origin of replication and termination sites, included in plasmids used for bacterial transformation for further use in transfecting mammalian cells.

Figure 0.5 is an extensive simplification of the plasmid used in the ligation reaction. Briefly, the reaction containing the sequences of interest was incubated on ice with the TOP10 *E. coli* cells and $CaCl_2$. The $CaCl_2$ increases uptake of the DNA sequence into the cells by aiding in the binding of the DNA to the cell by means of charge-charge interactions with the lipopolysaccharides on the outer membrane of the target host *E. coli*. Subsequently, the cells are subjected to a 30 second 42^{o} C shock, then immediately brought back to 37^{o} C and incubated for an hour, holding at this temperature. The heat shock is thought to allow the DNA to move through the cell membrane and thus be incorporated into the cell.

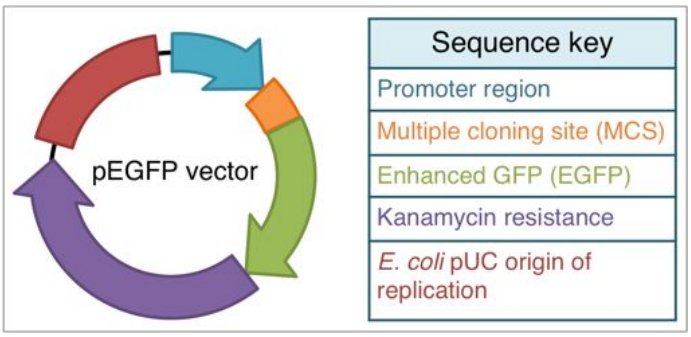

Figure 0.5: Simplified plasmid map of DNA used for transformation of *E. coli*. The map notes only sequences relevant to its function within our LbL system. The GFP region allows for mammalian cells to produce green fluorescent protein when successfully transfected with the pDNA in our experiments. The Kanamycin resistance region and *E. coli* origin of replication allow us to amplify this pDNA in *E. coli* grown in a Kanamycin environment to exclude other bacteria.

After incubation, the cell solution is spread on kanamycin Lysogeny Broth (LB) agar plates, incubated at 37^{o}C overnight, and a single colony is then removed from the plate with a sterile toothpick and placed into a small 5mL aliquot of Terrific Broth containing kanamycin. This aliquot is then allowed to incubate at 37^{o}C for 8 hours to allow the new, transformed, *E. coli* to reproduce. After the 8 hour incubation, this solution, referred to later as the "starter culture", can be used immediately for pDNA amplification and purification, or can be quickly chilled to 4^{o}C and reserved for use at a later time.

Amplification and purification

Terrific Broth (powdered; 11.8g SELECT Peptone 140, 23.6g yeast extract, 9.4 g dipotassium hydrogen phosphate, and 2.2 g potassium dihydrogen phosphate/L, Invitrogen) was prepared as directed, with 4 mL/L glycerol (Sigma) and autoclaved. 2 liters of the prepared broth were inoculated by diluting the starter culture 1/500 to 1/1000 supplemented with 1mL of 50 mg/mL frozen stock solution of kanamycin. The *E. coli* culture was grown at 37°C for 12–16 h with vigorous shaking (shaker speed set to approximately 180), using flasks with a volume of at least 2 times the volume of the culture. The bacterial cells were harvested by centrifugation following the protocol for Plasmid DNA Purification using the QIAGEN Plasmid Giga Kit. Following the kit protocol, the cells were lysed and filtered free of cell debris before being placed into the provided resin column which had been equilibrated for the binding and subsequent washing and purification steps to remove contaminants. After washing, the DNA was eluted from the column, precipitated by isopropanol, and separated by centrifugation. After removing the supernatant, the DNA was washed

Batch	#	260 (A)	260/280 (A)	260 (B)	260/280 (B)	*Min 260/280*
1		0.319	1.93	0.319	1.91	*1.791*
2		0.143	1.791	0.141	1.792	
3		0.114	1.915	0.113	1.923	*Max 260/280*
4		0.078	1.943	0.079	1.915	*1.976*
5		0.277	1.913	0.272	1.922	
6	1	0.422	1.917	0.424	1.906	*Ave. 260/280*
	2	0.422	1.901	0.429	1.906	*1.916*
7	1	0.226	1.915	0.225	1.917	
	2	0.119	1.938	0.12	1.921	*Min mg/mL*
8	1	0.085	1.942	0.087	1.976	*0.052*
	2	0.084	1.918	0.085	1.951	
9		0.114	1.908	0.113	1.948	*Max mg/mL*
10		0.142	1.904	0.138	1.909	*0.811*
11		0.139	1.911	0.14	1.915	
12		0.192	1.931	0.193	1.963	
13		0.053	1.934	0.052	1.952	
14		0.811	1.92	0.811	1.926	* diluted
	*	0.218	1.907	0.228	1.898	1:40

Figure 0.6: Spectrophotometric data for GFP-DNA. The yield in mg/mL is determined directly from the A260 measurements. As shown, yield (diluted 1:10 for increased sensitivity) significantly increased after transforming a new *E. coli* population.

by centrifugation with 70% ethanol to remove salts. The supernatant was removed, the pellet was dried and then the DNA was carefully re-suspended in increasing volumes of room temperature of 1x PBS until the pellet dissolved. Throughout this manuscript, the amplified and purified plasmid DNA product from using this protocol will be referred to as "GFP-DNA" for simplification and ease of use.

In order to determine the concentration and purity of the DNA produced, spectrophotometric readings were taken using a BioTek Synergy Multi-Mode Reader equipped with the Take3 Micro-Volume Plate. Briefly, the spectrophotometer recorded absorbance data for plain DI and duplicates of the samples diluted at 1:10 in DI water at wavelengths 260 nm and 280 nm. The background from the DI water samples was subtracted, and the ratio of the 260 nm reading to the 280 nm reading. The "A260/A280" ratio is an important estimation of purity. A value $\geq$1.8 is ideal for pure DNA and $\geq$2.0 for pure RNA. Deviations much lower than 1.8 could be indicative of different contaminants, either biological or chemical present in the plasmid DNA sample. A ratio higher than 1.8 is not indicative of any issues related to purity [43, 44]. BioTek cautions that the spectrophotometric reading at 260 nm occurs near the peak of the absorbance spectrum for nucleic acids, but that the reading at 280 nm occurs at a part of the spectrum that has a very steep slope, which could result in a very large discrepancy in the A260/A280 ratio from very small changes in the 280 measurement [45]. Both phenol contamination and protein contamination can lead to a lower A260/A280 ratio [43, 44]. Changes in pH are also shown to cause specific A260/A280 ratio shifts of 0.2-0.3 in either direction [43, 44]. From the data shown in table 0.6, the average A260/A280 ratio is 1.916, which is within the normal range for DNA with low contamination. [45].

Polyamidoamine synthesis

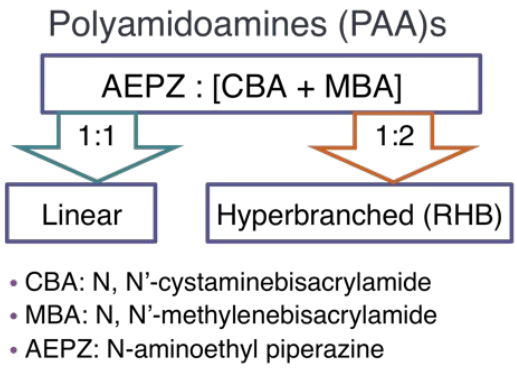

Figure 0.7: Left: Scheme of our linear versus reducible hyperbranched (RHB) polymers.

The main PAAs used in our experiments consisted of linear and reducible hyperbranched (RHB) disulfide-containing polymers. The raw materials are from Sigma-Aldrich and used as received (with the exception of CBA, which was recrystallized before use): 1-(2-Aminoethyl) piperazine (AEPZ, 99%), N,N´-Methylene bisacrylamide (MBA, 99%), N,N´-Cystamine bisacrylamide (CBA, $\geq$ 98%) , and 1-Methylpiperazine (MPZ, 99%). The disulfide-containing polymers were synthesized in house by Michael addition copolymerization of bisacrylamide monomers CBA and MBA to AEPZ in a 2:1 molar ratio (yielding RHB) or a 1:1 molar ratio (yielding a linear structure). APOL was synthesized in house using Michael addition of the "corresponding primary amine monomers [32]." For RHB, 1 mmol CBA (0.260 g), and 2 mmol MBA (0.308 g) were added to 1.5 mmol AEPZ (0.193 g) dissolved in 70% methanol in water (3.5 mL, v/v). Polymerization was carried out at 50 C for 5 or more days, on average. To consume any unreacted acrylamide groups, a minimal amount of 1-methylpiperazine was added, and the reaction was continuously stirred for 12 hours at 50 C. The polymer was obtained by using acetone to precipitate the final reaction mixture before it was dried at room temperature under vacuum. The dry products were brought to pH 3 by HCl and subsequently dialyzed against DI water. The final polymer solution was filtered in order to remove the upper and lower fractions and obtain a more uniform molecular weight. This was achieved through the use of Amicon Ultra-15 Centrifugal Filter Units with either the Ultracel-30 or Ultracel-3 cellulose membrane, corresponding to molecular weight cutoff of 30 kDa and molecular weight cutoff of 3 kDa, respectively. Afterwards, the solution was lyophilized in order to obtain the final desiccated polymer for use in polyplex and LbL film solutions.

Polyethylenimine (PEI) was used as received from Sigma Aldrich (branched, Mw $\sim$ 25 kDa,

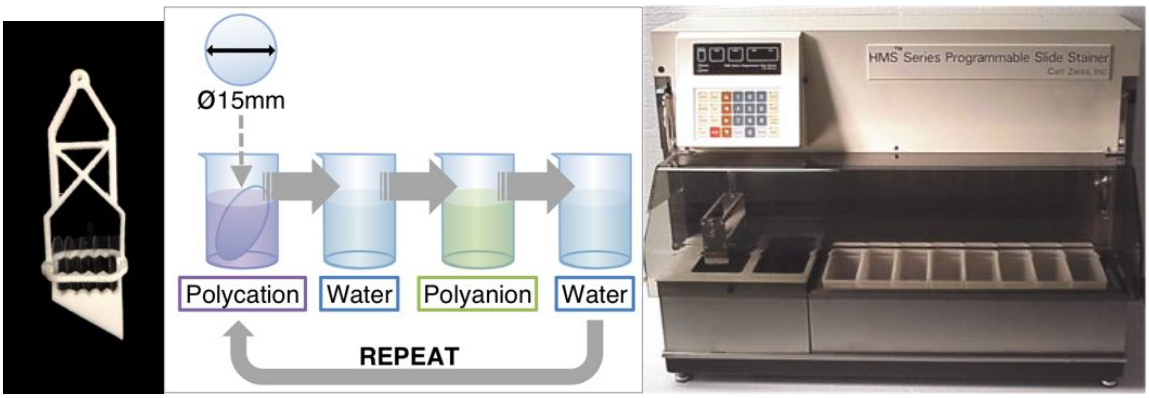

Figure 0.8: LbL dip-coating set up. Our LbL substrate is a 15 mm diameter round glass cover slip. Our molded plastic substrate holder can accommodate up to 5 substrates at once, and fits vertically inside a 5mL glass beaker placed at the bottom of a reservoir of the programmable slide stainer used to automate the dipping process. The entire set up includes 3 beakers (polycation, water, DNA) for Type A film construction or 4 beakers (polycation, PEI, water, DNA) for Type B film construction. As the slide stainer receives commands, it moves an arm horizontally to each prescribed location containing the beaker with aqueous solution, then lowers the substrate holder with substrate(s) vertically into the solution, submerging the substrate(s) and allowing the solution to come in full contact with all substrate surfaces. Photographs by Sean Carroll, with permission.

$\leq$ 1% water). In some cases, PEI was labeled with fluorescein isothiocyanate (FITC, 90%), or tetramethylrhodamine isothiocyanate (TRITC, 90%). Arginine-glycine-aspartic acid peptide-PEI (RGD-PEI) was a gift from Dr. Olivia Merkel's lab, College of Pharmacy and Health Science, Wayne State University. Hyaluronic acid sodium salt from human umbilical cord (HA, 95%) was used as received from Sigma Aldrich. All water used in synthesis, dilution, and reconstitution was deionized to 18 MΩ·cm resistivity using a Nanopure System from Barnstead.

Layer by Layer thin film assembly

Dip coating

Round glass slides (15 mm, Ted Pella) were stripped of impurities and cleaned using solutions of hydrochloric acid (HCl) and sulfuric acid (H_2SO_4). Briefly, glass slides were soaked in a mixture of methanol and HCl (v/v = 1:1) for 30 minutes, then immersed in 98% H_2SO_4 for another 30 min followed by rinsing with deionized water (Nanopure, 18 MΩ**.**cm resistivity).

The cleaned and dried glass substrates were dip-coated using a Carl Zeiss HMS50 programmable slide stainer with substrate holder made in-house that holds up to 6 substrates vertically (figure 0.8). Briefly from our previous work [46], the slide stainer took commands from a computer program that signaled the arm holding the substrate holder to lower into small, 5 mL beakers full of the component solutions at different locations in the apparatus at prescribed times. After a

specific amount of time, the program then methodically raised the substrate holder out of the component solutions, briefly paused and gently agitated, before moving on to the next sequence. The substrate deposition procedure started first with submersion in the polycation component solution (0.5 mg/mL with 30 mM pH 5.5 acetate buffer and 0.1 M NaCl) for 2.5 minutes followed by 3-1 minute DI water washes unless otherwise noted. The subsequent deposition solution/layer is the DNA polyanion solution (0.25 g/L with 30 mM pH 5.5 acetate buffer and 0.1 M NaCl), into which the slide stainer submerged the substrate for 2.5 minutes, unless otherwise noted. The polycation/polyanion deposition procedure was repeated until the quantity of layers desired was reached, generally 16.5 bi-layers. Figure 0.8 shows a simplified depiction of the process. Halfway through the dipping process, the procedure was temporarily halted and all of the solutions were discarded and replaced with fresh solutions to minimize carryover between solutions.

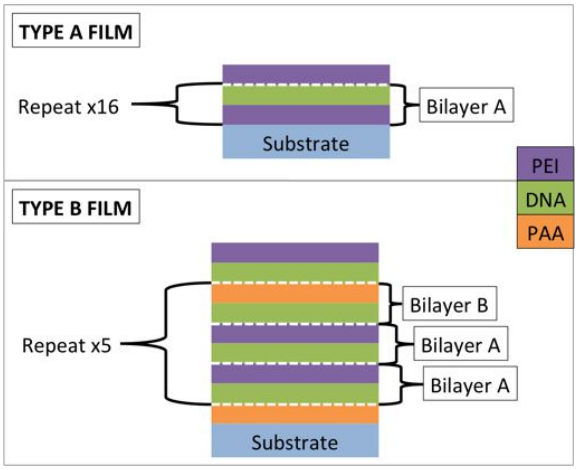

Figure 0.9: Type A versus Type B film structure

Chemical cross linking

Frequently, cross-linking the terminal layer of the bioreducible film was performed after the LbL buildup of the film on the substrate was complete. Briefly, the samples were cross-linked by allowing incubation in a layered cross-linking solution composed of 1 M 1,5-Diiodopentane (DIP, 97%), 5% hexane (both from Sigma-Aldrich), and deionized water at 50°C for 30 minutes. The sample was then removed, turned to the opposite side, and allowed to crosslink for an additional 30 minutes on the reverse side (unless otherwise specified, cross-linking was always performed on both sides of the sample). This ensured the entirety of the terminal surface of the samples were equally cross-linked. Samples were subsequently rinsed with ethanol and deionized water and dried before

using, or stored in deionized water in a closed container at 4 °C.

In vitro cell experimental set-up

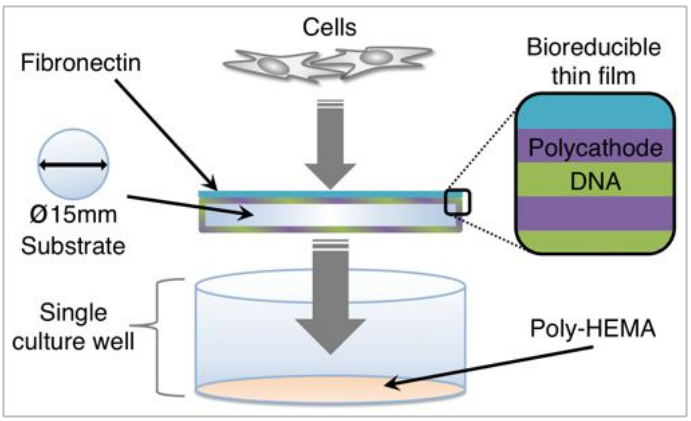

Figure 0.10: Schematic of in vitro experimental setup.

After cross-linking where applicable, the film-coated substrates are sterilized. Generally, ethanol sterilization is performed unless otherwise noted. Each sample is soaked in 70%-100% EtOH for 15 minutes in a glass receptacle to prevent adherence between the film and holding container. In sterile conditions, the substrates are then placed in sterile 1x PBS 3 times for 2 minutes each time. Each substrate is allowed to dry upright in sterile conditions for 15-20 minutes until dry, being careful not to allow it to adhere to the container. In sterile conditions, the substrate is carefully placed into a single well of a poly-HEMA -coated 24-well plate. LbL coated glass substrates are carefully placed parallel to the bottom of tissue-culture coated 24-well cell plates that have been treated with a thin, continuous layer of poly-HEMA (section). The diameter of the substrate is effectively identical to the well diameter, which provides a tight fit and minimizes the area available for cells to grow outside of the edge of the substrate. This ensures that the growing surface for the cells is kept as impartial as possible. For UV sterilization, the substrate is placed into the bottom of tissue-culture coated 24-well cell plates that have been treated with a thin, continuous layer of poly-HEMA and then placed into the tissue culture hood. A UV cleaning cycle is initiated (˜30 minutes), inside of a the closed tissue culture biosafety hood and seeding of the cells follows per protocol.

Following sterilization, a fibronectin coating is applied to the top of substrates, unless otherwise specified. In sterile conditions, 50uL of sterile 1x PBS is added to 40uL fibronectin (0.1% from human plasmid, Sigma Aldrich) and mixed well for each film. The substrate is covered with 90uL

of the mixture and allowed to dry, in sterile conditions, for at least 1 hour. Any excess is removed with a pipet and dried thoroughly before seeding cells on top of the surface. As seen in figure 0.10, after the poly-HEMA well/LbL coated substrate/fibronectin complex is complete, a cell/media suspension is applied to the top, and additional media is added to bring the total volume to ˜0.5 mL. Cell density is determined manually using a standard hemocytometer.

CHAPTER 3 RESULTS

DNA data & troubleshooting

Early on, DNA synthesis yields were extremely low. To troubleshoot, the DNA was tested by agarose gel. Briefly, a 1% agarose gel was prepared with ethylene bromide as a fluorescent nucleic acid stain. Plasmid containing GFP and our GFP specific plasmid were digested using Mfe1 and ACC1 restriction enzymes. Briefly, 5 µl plasmid and 1 µl of buffer were combined with 0.5 µl of each enzyme and 1 µl bovine serum albumin (BSA). The samples were placed in a thermocycler and run on a program holding the samples at 37 °C for an hour and then brought down to and held at 4 °C overnight. 4 µl of each of the samples were mixed with 2 µl loading dye (0.2% bromophenol blue in 50% glycerol) and run at 110 volts for approximately 10 minutes. In order to estimate size, a 1 kb molecular weight size marker "ladder", (1 kb Plus, Life Technologies) was run along with the samples. The digested samples were run on the agarose gel, and the results were consistent that the product was correct. therefore, we concluded that the low yield could very likely be due to a problem in the purification and amplification assay.

In order to analyze and confirm products from the DNA amplification and purification assay, an agarose gel was run. A protocol is provided with the Qiagen Gigaprep assay in order to evaluate the efficacy of the assay at various prescribed steps. Following the protocol, samples were collected from fractions at different time points during a single purification assay. For the agarose gel, briefly, a 1% agarose gel was prepared with ethylene bromide as a fluorescent nucleic acid stain. 2 µl plasmid were combined 2 µl loading dye and run at 110 volts for approximately 10 minutes. In order to estimate size, a 1 kb ladder was run along with the samples.

Sample A is collected after particulate waste should have been removed, and the cleared lysate should contain supercoiled and open circular plasmid DNA and degraded RNA and to determine whether growth and lysis conditions were optimal. Plasmid in open circular form (band A1) and supercoiled form (band A2) are shown in Figure 0.11 along with band A3 showing impurities and degraded RNA.

Sample B is collected after the DNA solution is passed through the resin filter column. This flow-through fraction should contain only degraded RNA and should lack plasmid DNA which should be bound and suspended in the Qiagen column and not passed through to the sample. Sample B determines the binding efficiency of the DNA to the resin. In figure 0.11, this is shown in the absence of bands B1 and B2 (open circular and supercoiled DNA. respectively) and the presence

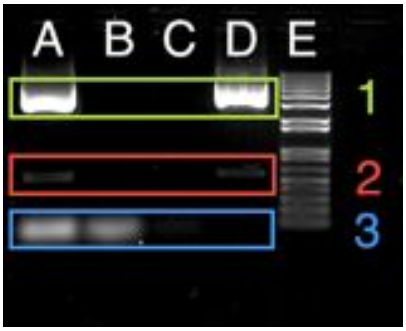

Figure 0.11: Agarose gel analysis for pDNA. At different stages during the purification process, fractions were collected and run in a 1% agarose gel containing ethidium bromide. UV microscopy was used to visualize the bands. Different features of the analysis are shown. The upper band (1) shows open circular form and the middle band (2) shows the supercoiled form of the amplified plasmid DNA in both the unpurified (A) and final purification (D) steps. The additional band (3) shown in the unpurified (A) step shows the degraded RNA impurity. This band is also present in the flow-through fraction (B) collected before washing the DNA, and a faint shadow of the band is seen in the flow-through fraction from the wash step (C). It is not present in the final purification step (D), indicating successful removal of the impurities.

of band B3 (impurities and degraded RNA).

Wash fractions were collected and combined for sample C. The remaining traces of RNA should be removed and seen in the sample, and the DNA should still be strongly bound inside of the resin column. This can be seen from the complete lack of bands C1 (open circular DNA) and C2 (supercoiled DNA) and dim band C3 (last of the impurities and degraded RNA washed out).

The DNA is then eluted from the resin column and the eluent is collected for sample D. At this stage, only the pure plasmid DNA with no other contaminating nucleic acids should be present. This is shown clearly in the bands D1 and D2 which are just as bright as the initial bands A1 and A2 before the contaminants had been removed. Not present is band D3 (contaminants) and an additional band directly below the supercoiled band (in between D2 and D3), which would indicate a DNA form resulting from prolonged alkaline lysis and is resistant to restriction digestion [QIAGEN Plasmid Purification Handbook — April 2012].

Even though having a stronger band of supercoiled DNA would have been ideal, all of the samples were as expected and there were no problems found within the amplification and purification process. In order to rule out proliferation of a bad batch of bacteria or sub-par growth conditions, fresh *E. coli* was plated and the amplification and purification process was restarted. Unfortunately, this produced the same positive results, so we started from the ground up by re-transforming the bacteria, this time using a different, confirmed TOP10 chemically competent *E. coli*. After making this change, the yield went up significantly from about 0.1 - 0.3 mg/ml to approximately 0.8 mg/ml.

Layer-by-layer buildup and degradation measured with AFM

AFM was used to measure film thickness and film features such as surface roughness. A Dimension 3100 AFM from VEECO was used in tapping mode in air with silicon probes (VEECO) with a nominal frequency of 150 kHz. Film thickness was measured using a razor-blade cut method. Complete films were scored in multiple intersecting straight lines, removing the film in those areas and exposing the glass substrate. The distance between the top film layer and the bottom glass substrate are then measured using AFM using sectional height analysis. In order to obtain an average, multiple areas were measured. From our previous work [46], "the film surface roughness is the root mean squared roughness $RMS = [\sum(z_i^2/N)]^{1/2}$, where z_i is the height value of each measurement point and N is the number of measurement points in AFM height images. All RMS values reported were obtained on an area of 5 × 5 μm2. AFM tapping mode in liquid was used to monitor film degradation in situ in 50 μL of 20 mM DTT in phosphate buffered saline (PBS, pH 7.4) containing 137 mM NaCl, 2.7 mM KCl, 10 mM Na_2HPO_4, and 2 mM KH_2PO_4 at room temperature using silicon nitride probes (NP type, VEECO) with a nominal radius of curvature of 20 nm and a nominal cantilever spring constant of 0.38 N/m. AFM imaging ensued immediately after DTT solution injection. The surface was imaged continuously at an average rate of 1−2 Hz until no significant changes were observed. The ranges of frequency, amplitude, integral, and proportional gains used are 7−9 kHz, 0.5−1 V, 0.5−2, and 0.75−3, respectively."

As shown in figure 0.12, thickness was measured to determine the influence of both cross-linking and extracellular matrix interactions on film thickness before and after having cells cultured on the surface for in vitro experiments. Figure 0.13 shows the influence of layer thickness due to a modified polyanion layer consisting of a DNA/HA blend. Again, the films were examined before and after having cells cultured on them for in vitro experiments and there is clear evidence of cellular interactions with the film surface.

In vitro transfection

Preliminary experiment

In order to gain familiarity, the cell culture and preparation steps of the first experiment were completed in Dr. Ren's lab, using equipment and supplies under supervision of lab personnel. A single "normal" (16.5 bilayers) Type B film was made, using 100% linear PAA. The film was cross-linked using standard DIP cross-linking, for 30 minutes per side before placing in a 6-well

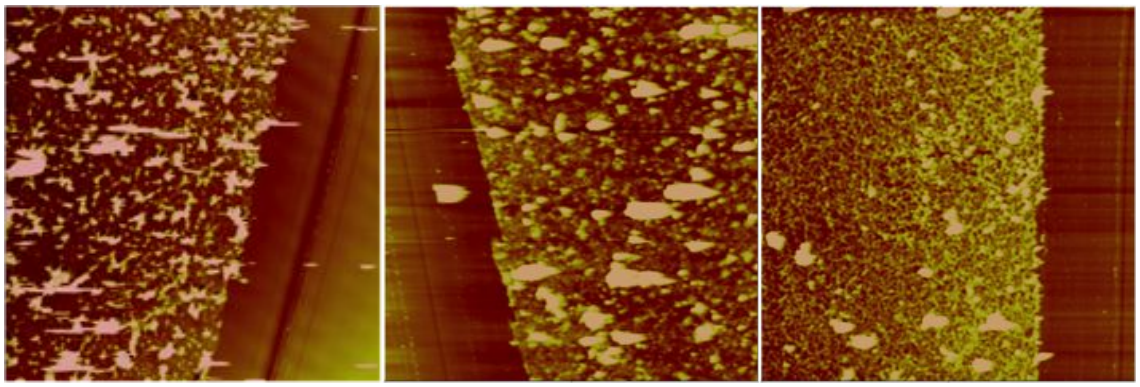

Figure 0.12: AFM images. Cross-linked Type B films influenced by cellular attachment. Before and after culturing cells for 14 days. As shown, the thickness changes significantly, from 54nm before culture, to 29.2 nm (MC3T3 cells) and 38.1 nm (HEK-293 cells) after. Pre-cell film (left), after MC3T3 cells (center), after HEK-293 cells (right).

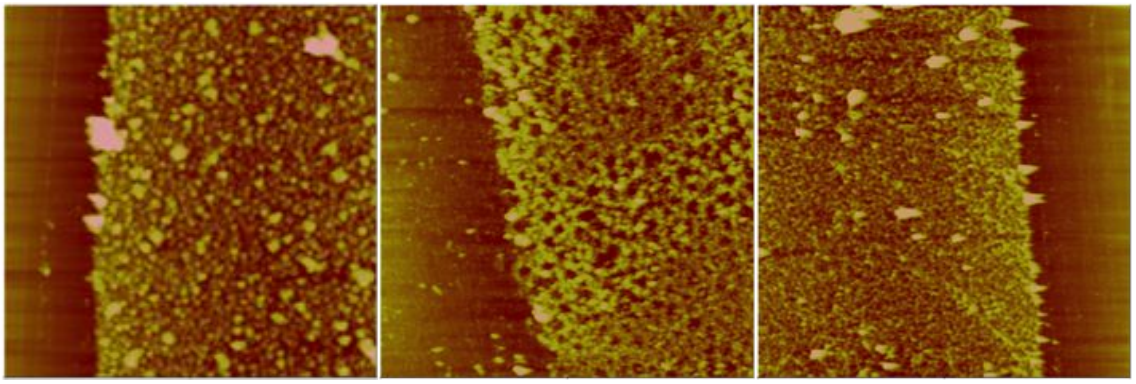

Figure 0.13: AFM images. 1:4 DNA:HA anion layer Type B films influenced by cellular attachment. Before and after culturing cells for 14 days. The pre-cell film (left) looks much smoother and have more uniform particle size than the cross-linked pre-cell film found in figure 0.12. The pre-cell thickness of the film is 68.2 nm, and after 14 days, is 25.4 nm (MC3T3) and 19.2 nm (HEK-293). Pre-cell film (left), after MC3T3 cells (center), after HEK-293 cells (right).

poly-HEMA coated cell culture plate pre-made by the Ren laboratory. The film, placed inside of the culture dish, was UV sterilized overnight using the sanitization cycle of the cell culture hood before seeding cells. The cells that were available were the RAW macrophage cell line, and 50,000 RAW cells were seeded onto the film in the culture plate before covering the film with culture medium and allowing to grow in standard culture conditions mentioned in methods section .

Brightfield and fluorescence microscopy was performed after 1 week. Figure 0.14 shows the best brightfield image obtained. For a few rare cells, the presence of multinucleated morphology suggested foreign-body giant cells. It was hypothesized that there may have been a minute transfection response, and that the foreign-body giant cells were responding to intake of foreign LbL material. No fluorescence micrographs are shown, as they were featureless, showing conclusive lack of GFP expression. Cells were cultured for 10 days total. Cells grew mainly on the film surface, but the size

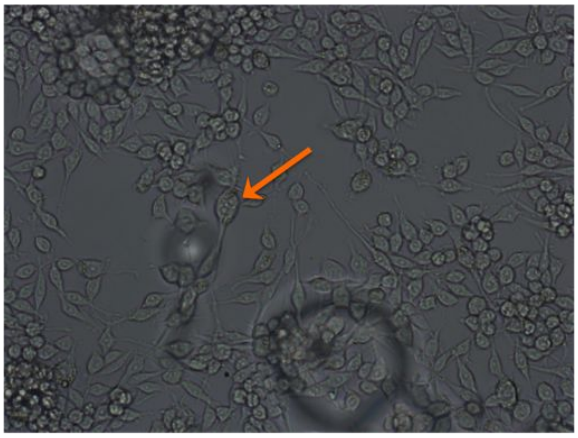

Figure 0.14: Brightfield image 20x, RAW cells after culturing for 1 week. The orange arrow indicates a multi-nucleated cell, which could be a foreign-body giant cell, formed in response to LbL film component uptake. No GFP expression was found.

difference between culture plate edge and the film edge provided unnecessary surface area for the cells to grow, and also consumed more raw materials than a culture plate conforming to the size of the film would have. It was determined, for future experiments, a 12-well plate having less surface area would be utilized. Additionally, no positive control was utilized, and as such, the transfection capability of the GFP-DNA, synthesized by an alternate lab personnel, was unknown.

Type B films with hyaluronic acid (HA)/DNA blend polyanion layer

A number of variables were introduced in experiment 2, which consisted of four distinct Type B films. Each film was broken into 3 pieces in order to use a single piece for each of 3 cell lines, RAW, NIH/3T3, and HEK-293. This yielded 12 total samples. PAA was 100% linear and conjugated with FITC for use in further fluorescence microscopy applications (not performed). Film 1 was normal Type B films with 16.5 bilayer construction (100% linear FITC-PAA, PEI, GFP-DNA). Film 2 was a 17 bilayer film with base of normal Type B 16.5 bilayer construction (100% linear FITC-PAA, PEI, GFP-DNA), and an additional single terminal layer of PAA/DNA polyplex. Due to its enhanced transfection capability, this polyplex layer film should act as a positive control. Film 3 was the same normal Type B 16.5 bilayer film with the terminal FITC-PAA layer subjected to 30 minutes of chemical cross-linking (described in section) on both sides. Film 4 was a 16.5 bilayer film with a modified polyanion DNA layer (100% linear FITC-PAA, PEI, 1:3 blend of HA:GFP-DNA). Hyaluronic acid (HA) is an extracellular matrix component, and is involved in cell migration/proliferation, and by combining it in our LbL structure, it was hoped that cells would

be attracted to and encouraged to interact with the films, thus promoting transfection.

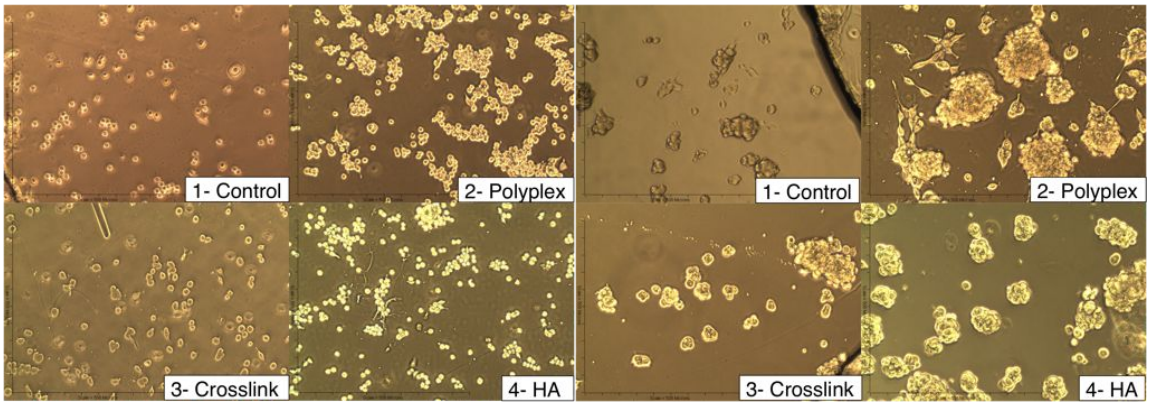

(a) RAW cells

(b) NIH/3T3 cells

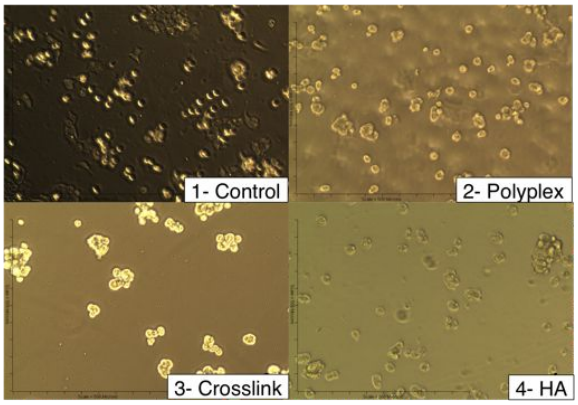

(c) HEK-293

Figure 0.15: Brightfield images showing the different cell types one day after culture on the LbL films. Cells all did not attach well, and are present on both the film and the culture plate. No GFP expression was found after 14 days.

Fluorescence and brightfield microscopy was performed at 1, 6, 10, and 14 days after the 50,000 cells of each cell line were seeded on the films. As shown in figure 0.15, none of the 3 different cell lines attached or spread well onto the films after a day of culture. This indicated that for future experiments, the terminal layer of the film, in contact with the cells, should be altered in order to enhance cell attachment and growth, thus facilitating transfection and GFP expression.

As time progressed, the cells preferentially aggregated and favored the irregular, exposed-glass edges of the broken slides. Cells grew on both sides of the films, regardless of the fact that the plate was coated with the anti-cellular attachment agent, poly-HEMA, making obtaining clear micrograph images of one single plane difficult. The cells also grew on the plate outside of the sample area. Since

the samples were placed in a 12-well plate, the area around the samples was still significant, spanning an area of around 2 times the area occupied by the sample. This extra space caused problems as the samples moved freely around the plate, and in some cases, the samples were found free-floating in the media at the time of observation for microscopy. It was determined that a smaller surface area might be employed (24 well-plate), and that the samples should absolutely not be broken into multiple pieces, as it compromised the integrity of the experiment by providing preferential growth surfaces and altered the interaction of the cells with the film surface. Eventually, cells (NIH/3T3 shown in figure 0.16), attached well, although not uniformly, and after 10 days, complete confluence was achieved that became overgrown at day 14. Unfortunately, this attachment, although on many surfaces, and preferentially at the cell edges, there was no GFP expression at any timepoint. No fluorescence micrographs are shown, as they were black and featureless, showing conclusive lack of GFP expression for all samples. Although RAW cells are a "suitable transfection host" according to ATCC, their lack of transfection and lack of utility for future applications excludes their use in any further in vitro experiments.

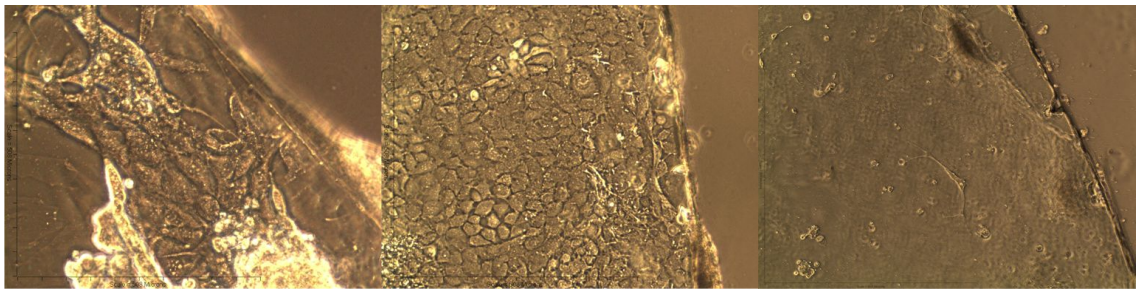

Figure 0.16: Brightfield. Progression of NIH/3T3 cell growth on Type B film, no cross-linking. Day 6 (left), day 10 (center), and day 14 (right). No GFP expression was found after 14 days.

Of note, the samples that contained the film with modified polyanion layer of 1:3 HA:GFP-DNA ratio seemed healthier and more stable by visual inspection. This finding encourages use of hyaluronic acid in further approaches. Interestingly, a number of artifacts were observed as shown in the microscopy samples in figure 0.17. Symmetric rings, approximately 30-60 microns in diameter, reflecting light are shown in clusters on samples of multiple cell lines and film types. It is unknown what caused these irregularities, but since they were observed across multiple different sample types, it may have been some sort of gas bubble created between the two interfaces, or an interaction between the film surface and the poly-HEMA culture plate. It is unclear from the micrographs what plane the defects are on.

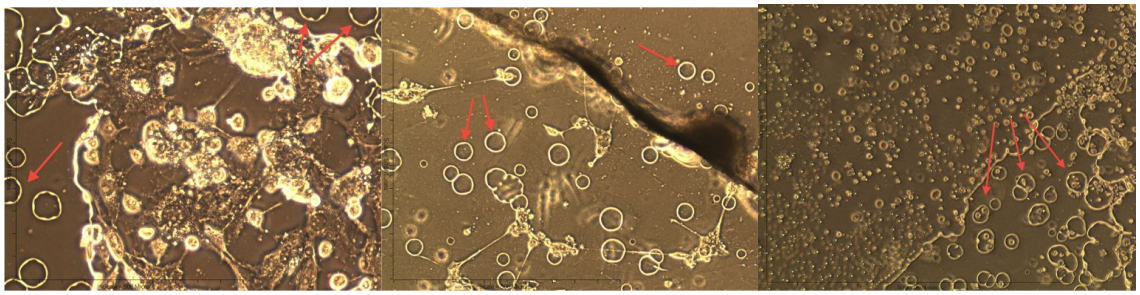

Figure 0.17: Brightfield. Ring-like irregularities: Day 6: Polyplex terminal layer film with NIH/3T3 cells (left), Day 10: Cross-linked terminal layer film with NIH/3T3 cells (center), Day 14: Control film with RAW cells (right). No GFP expression was found after 14 days.

Polyplex transfection with RHB and PolyJet control.

The preliminary polyplex experiment investigated the transfection potential of RHB on two cell lines, RAW and HEK-293. The experiment also compared the transfection efficiency of the commercially available PolyJet agent and our homemade polyplexes consisting of a 4:1 w/w RHB:GFP-DNA. The original intent was to include all available cell lines (NIH/3T3, HEK-293, and RAW), but the growing conditions appeared sub-optimal for the NIH/3T3, and their sharp decline in health precluded their testing for this polyplex experiment.

For our RHB polyplex and PolyJet procedures, cells are plated 18 to 24 hours prior to transfection in order to reach optimal confluence (at least 70˜80%). Medium is exchanged 30-60 minutes before the transfection begins, and the polyplex or PolyJet colloid solutions are prepared using either polymer (RHB in this case) or PolyJet reagent vortexed with our GFP-DNA in the prescribed ratio. The mixture is allowed to incubate briefly at room temperature and then used immediately. The polyplex or PolyJet mixture is added to the prepared cells and evenly distributed throughout the sample my mixing. After incubating at standard cell culture conditions for 3-4 hours (our polyplex) or 12-18 hours (PolyJet). The medium is then exchanged and the cells are incubated for another 24+ hours before confirming transfection using fluorescence microscopy to measure GFP expression. As is shown in figure 0.18, widespread transfection was achieved for the PolyJet samples for both cell lines. Interestingly, the fluorescence of the HEK-293 cells was significantly brighter and more pronounced than that of the NIH/3T3 cells. The widespread and vivid GFP expression encourages the use of this cell line for future experiments, as it seems to be very receptive to transfection.

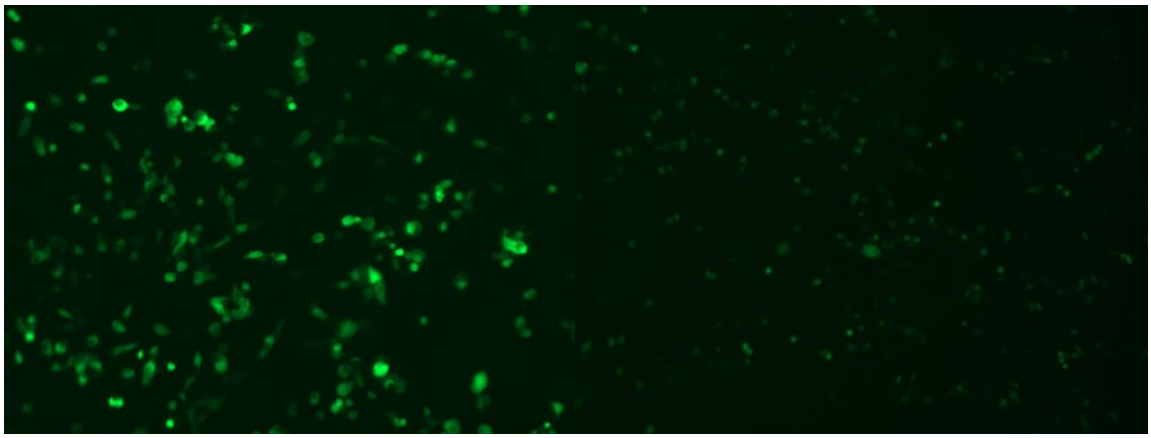

(a) PolyJet: HEK-293 cells (left) and RAW cells (right) widespread GFP expression.

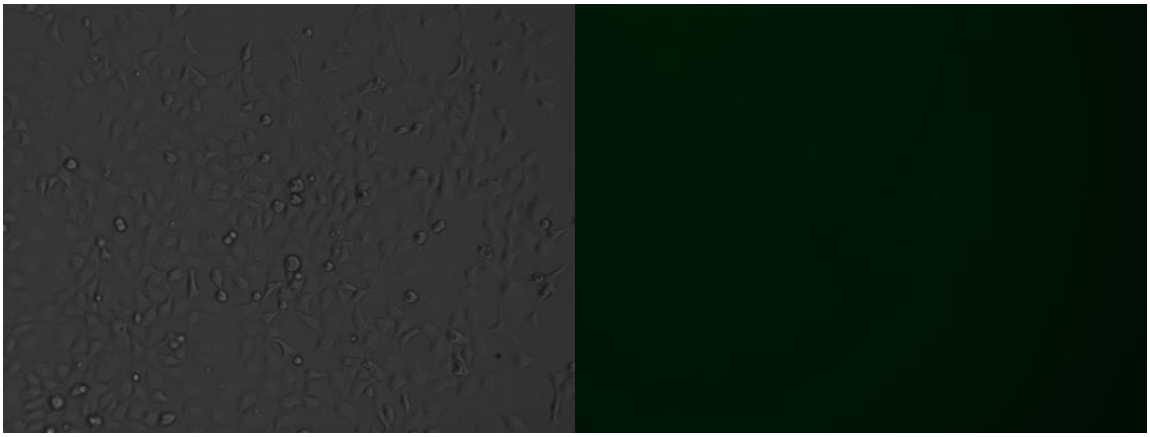

(b) RHB polyplexes: HEK-293, brightfield (left) and GFP channel (right)

Figure 0.18: GFP expression and transfection: comparison of our first RHB polyplex vs. PolyJet. 10x.

Type B films with PAA/DNA polyplex top layer and a DNA/HA blend polyanion layer

Because of the high incidence of transfection from the HEK-293 cells, the next experiment used only this cell line in order to test a normal. Film 1 was a normal 16.5 bilayer Type B film with PEI, TRITC-labeled 100% linear PAA, and a DNA:HA 3:1 blend for the polyanionic layer. The terminal layer was cross-linked for 30 minutes. Film 2 is a 17 bilayer film, with a base of normal 16.5 bilayer Type B film, and an additional 0.5 bilayer of a DNA/TRITC-labeled 100% linear PAA polyplex layer. Day 4 images, as shown in figure 0.19, reveal islands of cells with poor attachment and spreading for film 1, while film 2 with the polyplex top layer has almost confluent, well-attached and spread cells. It could be possible that the extended cross-linking time of 1 hour for film 1 caused too rigid of a surface environment for the HEK-293 cells. Regardless, there was no transfection for either samples after 4 days. Figure 0.20shows day 6 images for the polyplex

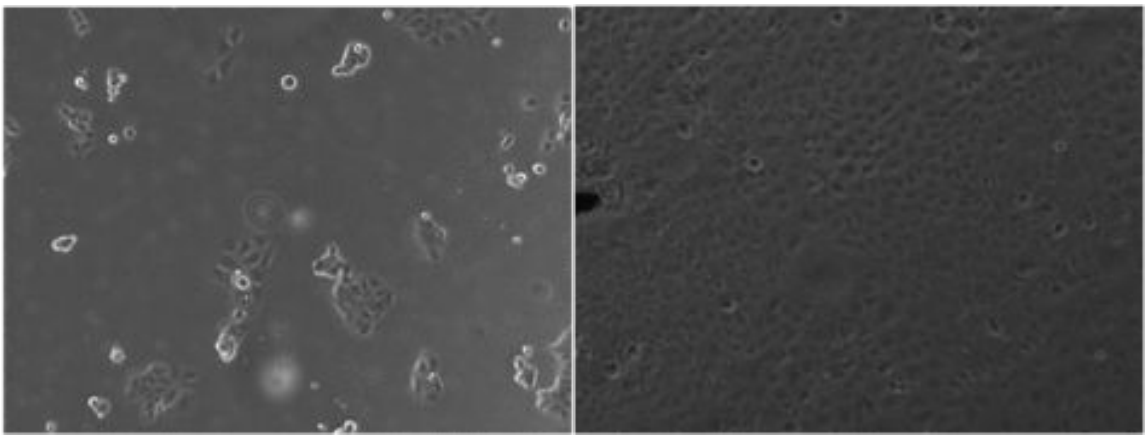

Figure 0.19: Day 4 brightfield images, HEK-293, 10x. 1 hour cross-linked Type B film with DNA:HA blend (left) and non-cross-linked Type B film with PAA/DNA polyplex top layer (right). After 4 days, the cell attachment and spreading is markedly different.

top layer film 2 only. The brightfield image shows confluent cells that are spread and healthy and the fluorescent image shows 2 very bright green cells showing successful transfection. The lack of widespread transfection raises concern, as these were the only two cells of the entire sample that fluoresced. The poly(HEMA) was dried overnight, as irregularities in the poly(HEMA) surface in the previous experiment caused concern that perhaps insufficient drying time caused the coating to be compromised and allow cells to grow on both sides of the samples. Figure 0.21 shows brightfield images from end-of-experiment (2 weeks), there was no evidence of transfection, so fluorescence images are not shown. Both images are the polyplex film. Cells were so overgrown that they formed a carpet of cells with odd morphologies in some places, and completely sloughed off in many other places on the film. Because of their successful transfection, even for two cells, polyplex top layers will be examined in future experiments.

Exploring transfection of MC3T3 cells using Type A and Type B architectures

In order to focus on the transfection of the preosteoblast MC3T3 cell line, Type A and Type B architecture films with modified dipping times of 10 minutes were fabricated using a DNA:HA 3:1 (w/w) polyanionic layer. The PAA used was 100% linear. Both films were cross-linked for 30 minutes per side and terminated with a fibronectin layer. Fibronectin should enhance cellular recognition and interaction between the film surface and the cell. In order to optimize growth conditions, 10,000 less cells than previous experiments were used in hope that overgrowth and sloughing could be avoided (40,000 cells total). In figure 0.22, brightfield images shown only, as

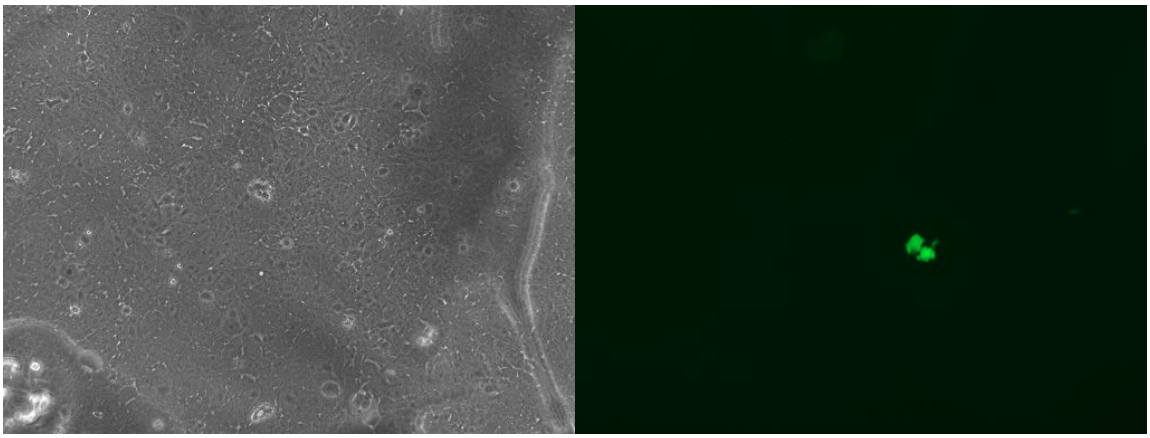

Figure 0.20: Day 6 images brightfield (left) and fluorescence (right), HEK-293, 10x. Type B film with PAA/DNA polyplex top layer. Brightfield image shows excellent cell spreading and fluorescence image shows a single isolated transfection of two healthy cells. GFP expression was not widespread.

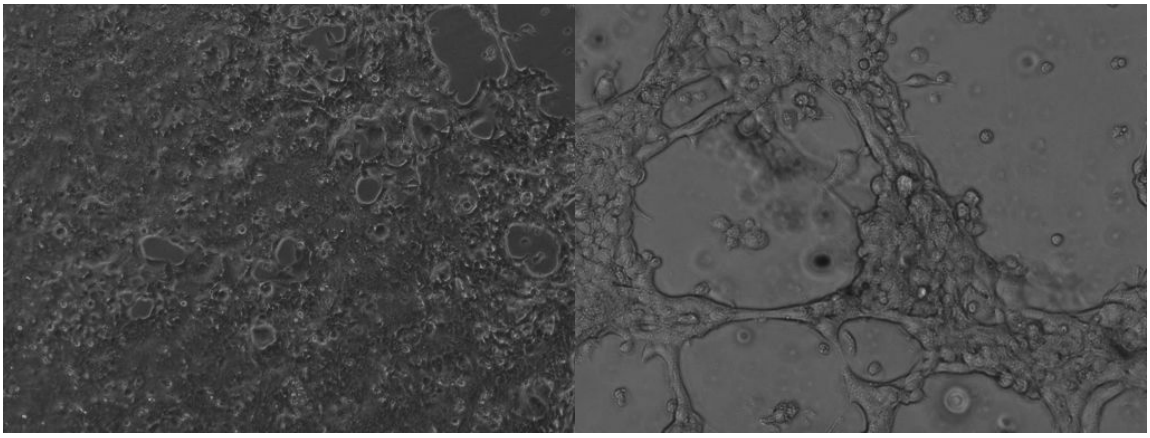

Figure 0.21: Day 14 images, brightfield, HEK-293, 10x. End-of-experiment, both images are the Type B film with PAA/DNA polyplex top layer. Cells are overgrown, and unhealthy, displaying odd morphologies in some places, and completely sloughing off in many other places on the film. No GFP expression was observed.

fluorescence data were vague, showing a faint green blush in 1 total cell for Type A film after 6 days, and 2 total cells for Type B film after 4 days. Despite cells attaching and spreading very well and looking generally healthy (likely due to the fibronectin), widespread or strong GFP expression was not seen. The thickness of the layers due to longer dipping time may have played a role in transfection, but evidence was inconclusive.

Group 2: RGD-PEI films: cross-linking vs. non cross-linking

We hypothesize that the polymeric constituents being used are sufficient for transfection and that cell attachment and spreading could be optimized, increasing transfection. Previous work indicates that coating the top of the thin film surface with fibronectin enhances the contact between cell and

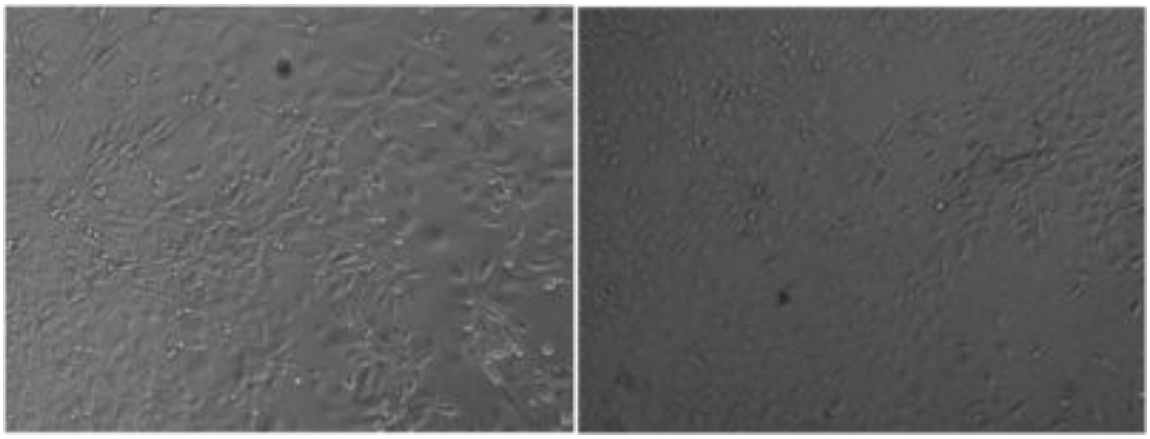

Figure 0.22: Day 10: Type A vs. Type B films, DNA/HA polyanionic layer, cross-linking for 30 minutes, fibronectin top coat, MC3T3, 10x. Brightfield images shown only, as fluorescence data were inconclusive. Cells attaching well and looking generally healthy, likely due to fibronectin.

substrate. The tripeptide sequence arginine-glycine-aspartic acid (RGD) is present on a number of extracellular matrix proteins including fibronectin. It is known to "mediate cell attachment directly when presented to cells as an insoluble substrate" [47]. Therefore, we examined the effects of adding RGD into our Type B film architecture. We chose to combine it with our PEI layer, synthesizing a conjugate referred to as "RGD-PEI" for simplicity. This RGD-PEI replaced the PEI layer in the normal 16.5 bilayer Type B film. The PAA used was 100% linear, 100% CBA. The DNA used was a 3:1 (w/w) DNA:HA blend. The top layer was coated with fibronectin prior to cell seeding but after chemical cross-linking for the samples that are indicated as such. As this experiment was a proof of concept, samples were not run in multiples, and only HEK-293 cells, which have shown higher, more reliable transfection.

The three samples were as follows: Type B RGD-PEI/3:1 DNA:HA/100% linear PAA 1) cross-linked and 2) non-cross-linked, and Type B PEI/3:1 DNA/HA/100% linear PAA 3) cross-linked "control". Transfection was present at day 2, and peaked for 1) the cross-linked RGD film between days 4 and 6 as seen in figure 0.23a, but at day 10 there was complete absence of GFP expression. Although GFP expression is absent at day 2, transfection showed at day 4, and peaked for 3) the cross-linked "control" between days 6 and 10, shown in figure 0.23b. Throughout the experiment, there was lack of transfection for 2) the RGD-PEI without cross-linking shown in figure 0.23c. Using 40,000 cells seemed to relieve most of the overcrowding issues, although at day 10 there were still a few areas that looked as if sloughing was occurring. There was no transfection with the non-cross-linked RGD film and also there were very little signs of a healthy cellular environment–the cells did not attach well, nor did they spread well. Over multiple days rounded, clumps of cells were

observed, indicating poor attachment. Since this film was not cross-linked, clearly cross-linking plays a very important role for the HEK-293 cells, even in the presence of fibronectin and RGD. The success of introducing RGD-PEI into the Type B film architecture shows promise for using it, in conjunction with fibronectin and cross-linking, for other cell lines and new PAA formulations and other experimental polycations. Everything can be seen shown in figure 0.23

Type A film repeat and Cy-5-labeled DNA films for microscopy

Type A architecture film with modified dipping time of 10 minutes was fabricated using a DNA:HA 3:1 (w/w) polyanionic layer, this time with the HEK-293 cell line instead of the MC3T3 cell line used before. The PAA used was 100% linear, 100% CBA. The top layer was coated with fibronectin prior to cell seeding but after chemical cross-linking (30 minutes). Only 1 sample was prepared. Additionally, a Type B film, with TRITC-labeled PAA and Cy-5-labeled DNA was fabricated, for future use in confocal microscopy. This sample was created in duplicate, and one of each film was used for the HEK-293 cell line and the MC3T3 cell line. Samples were cross-linked for 30 minutes per side and topped with fibronectin. Again, 40,000 cells were used to relieve overcrowding. Unfortunately, by day 4 (figure 0.24a and figure 0.25, left), cells on all samples were unhealthy, detaching from the plate and appeared shriveled. Over the next 4 days, the cell health did not improve (see day 6 images, figure 0.24b and figure 0.25, right), and many cells were washed away upon regular replacement of media. There was no GFP expression at any timepoint, and due to the extreme cell issues, this experiment was deemed inconclusive. The consistent degradation of cell health suggests possible environmental stress. This was later partly attributed to complications with the humidity in the incubator.

Comparison of cross-linking times, using Type A films and HEK-293

In order to understand the relationship between surface stiffness and transfection, a side-by-side comparison of two different cross-linking conditions was conducted, using only the HEK-293 which have better transfection chances. The PAA used was 100% linear, 100% CBA. The top layer was coated with fibronectin prior to cell seeding but after chemical cross-linking for 30 minutes per side (film 1) or 60 minutes per side (film 2). Only 1 sample of each type was prepared. In order to further reduce overcrowding 10,000 less cells were used (30,000 total). Despite excellent attachment after 2 days (slightly enhanced attachment from the 1 hour cross-linked sample, (figure 0.26, left),

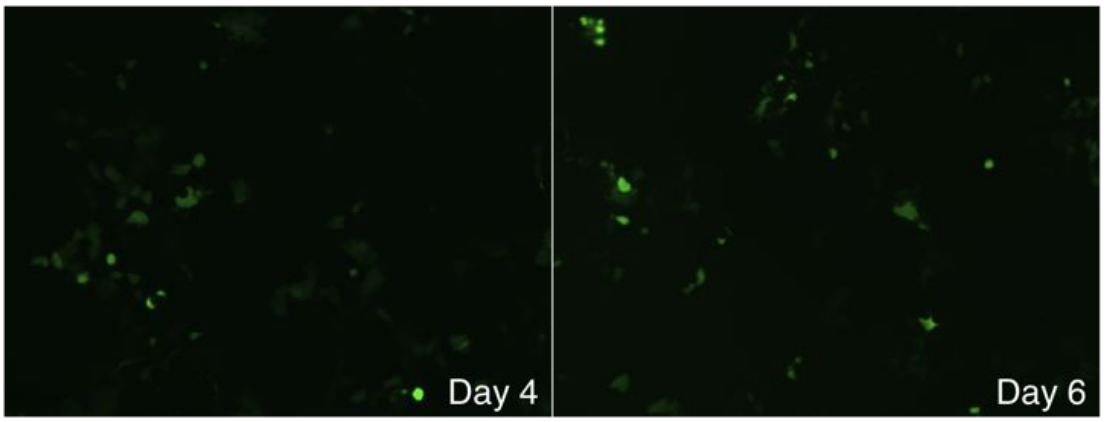

(a) RGD-PEI Type B film cross-linked with HEK-293 cells; peak expression, days 4 and 6.

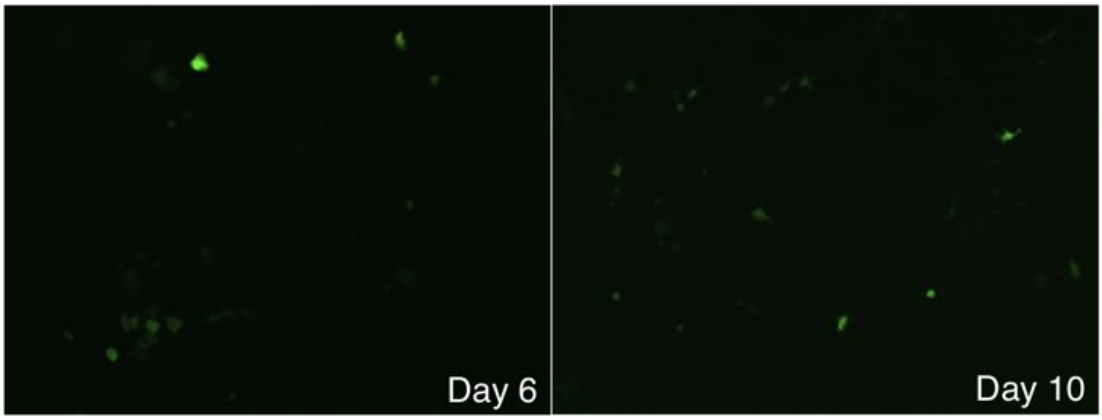

(b) Type B film cross-linked "control" with HEK-293 cells; peak expression, days 6 and 10.

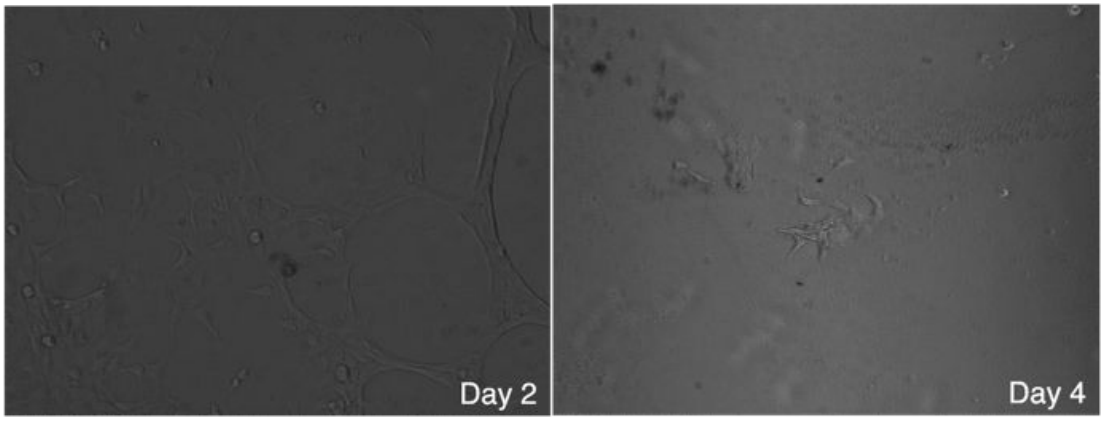

(c) RGD-PEI Type B film without cross-linking. Lack of transfection indicates cross-linking may play an important role in the health and transfection of the HEK-293 cells.

Figure 0.23: Testing the effects of RGD, a known tripeptide to enhance cellular recognition on transfection in Type B film architectures with and without cross-linking. a) Type B RGD film cross-linked and b) Type B non-RGD cross-linked. Both cross-linked samples show transfection, with GFP expression peaking over several days. Non-cross-linked Type B RGD film did not transfect, and cell health looked compromised, even with the presence of fibronectin and RGD. This suggests a relationship between cross-linking, RGD, and transfection for HEK-293 cells.

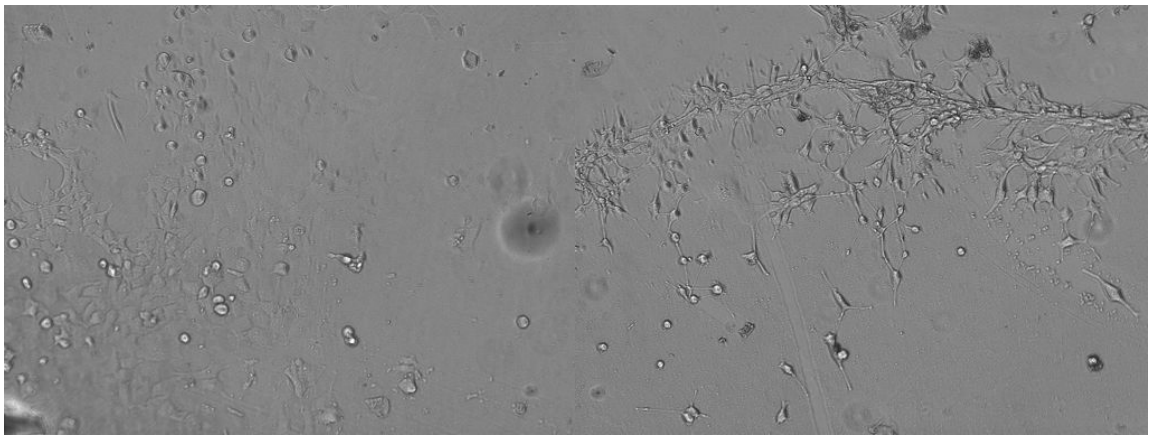

(a) Day 4 brightfield images, Type B films with Cy-5 labeled DNA and TRITC-labeled PAA. HEK-293 cells (left) and MC3T3 cells (right). Poor spreading and rounded morphology for both cell lines suggests problems. No fluorescence data shown, no GFP expression. 10x magnification.

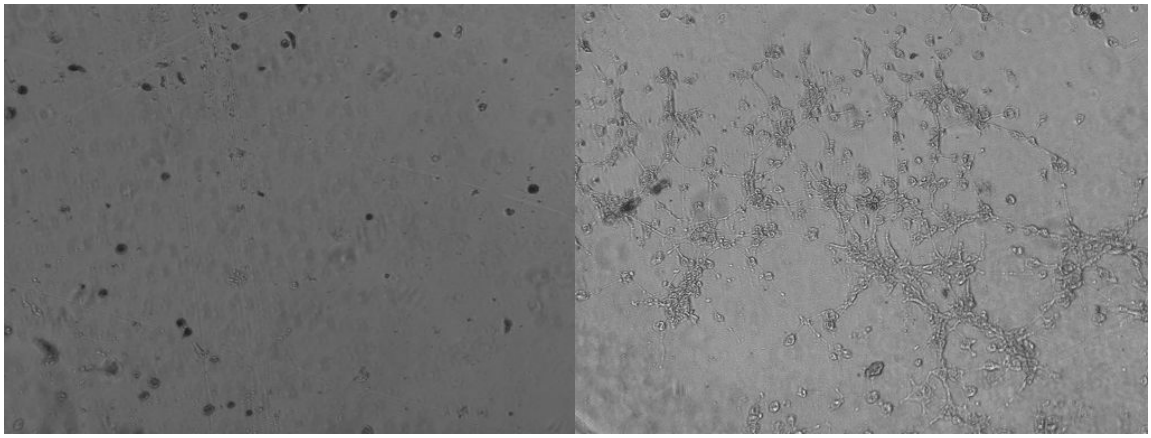

(b) Day 6 brightfield images, Type B films with Cy-5 labeled DNA and TRITC-labeled PAA. HEK-293 cells (left) and MC3T3 cells (right). Both cell lines show signs of cellular distress. No fluorescence data shown, no GFP expression. 10x magnification.

Figure 0.24: Type B films

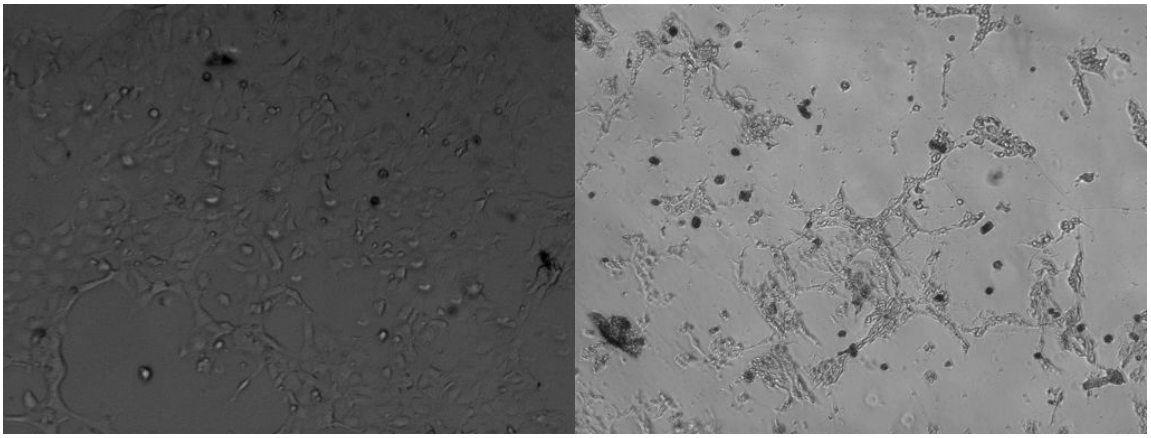

Figure 0.25: Type A re-do film using HEK-293 cells, a 1:3 DNA:HA polyanionic layer and a 10 minutes dipping time. Day 4 (left) and day 6 (right) brightfield images. Day 6 results show clear indications of poor health. No fluorescence data shown, no GFP expression. 10x magnification.

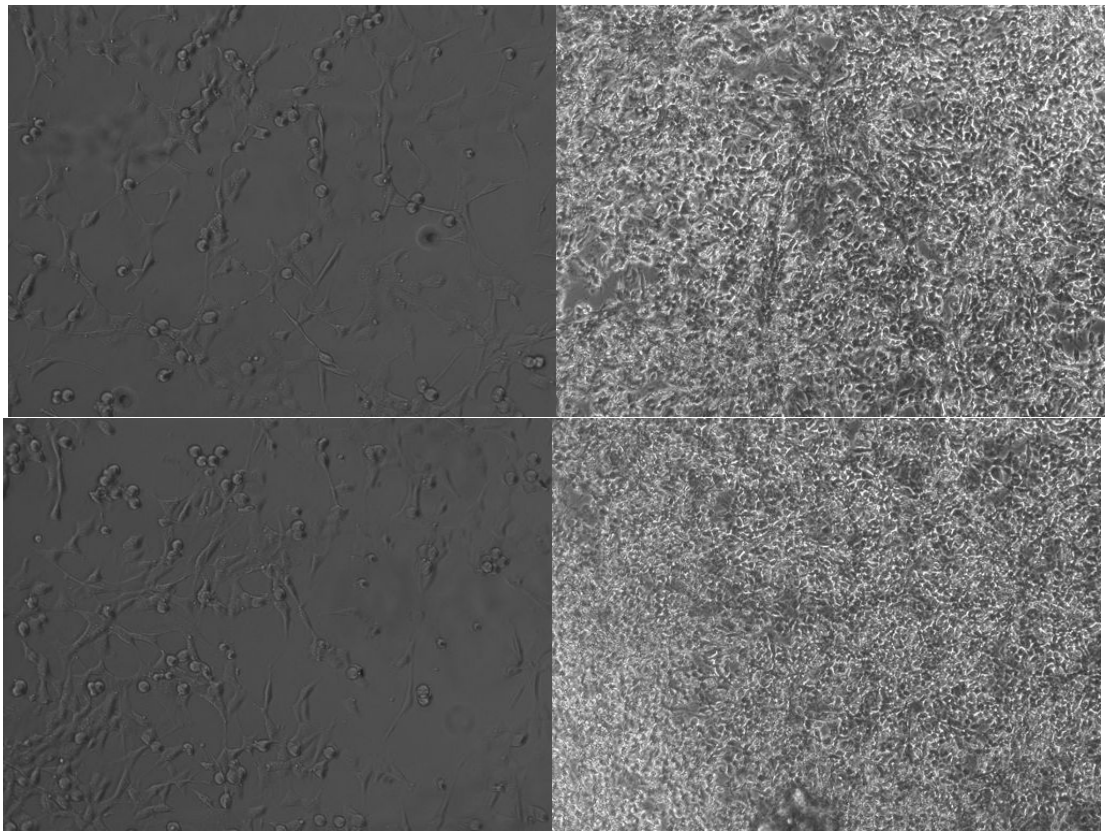

Figure 0.26: HEK-293 cells, 30,000, 10x magnification. 30 minutes cross-linking (top) and 60 minutes cross-linking (bottom). Left shows day 2 healthy cells; right shows day 8, complete confluence, overgrown. Overgrowth continued through day 10, end of experiment. No fluorescence data shown, no GFP expression.

no GFP expression was found for either sample. After 6 days, the cells were both in excellent health and grew so well that they were experiencing overgrowth at only 8 days (figure 0.26, right) with reduced cell count, there was still no GFP expression for either sample. Although this suggests that longer cross-linking time may aid in cellular interaction with the film but not facilitate transfection, there was also no positive control for this experiment to confirm this hypothesis.

Electrospun poly (ε-caprolactone) (PCL) nanofiber substrates

In a collaboration with Dr. Ren's lab, glass substrates were first coated with poly (ε-caprolactone) (PCL) nanofibers using electrospinning techniques. These nanometer-scale fibers made of biocompatible and biodegradable polymer are randomly oriented and provide increased surface area and enhanced porosity [48]. The nanofiber substrates were then dip-coated to create Type B LbL films on top. We hypothesize that this enhanced surface environment will greatly increase cellular interaction and result in increased attachment and growth. For this reason, we reduced the cell seeding

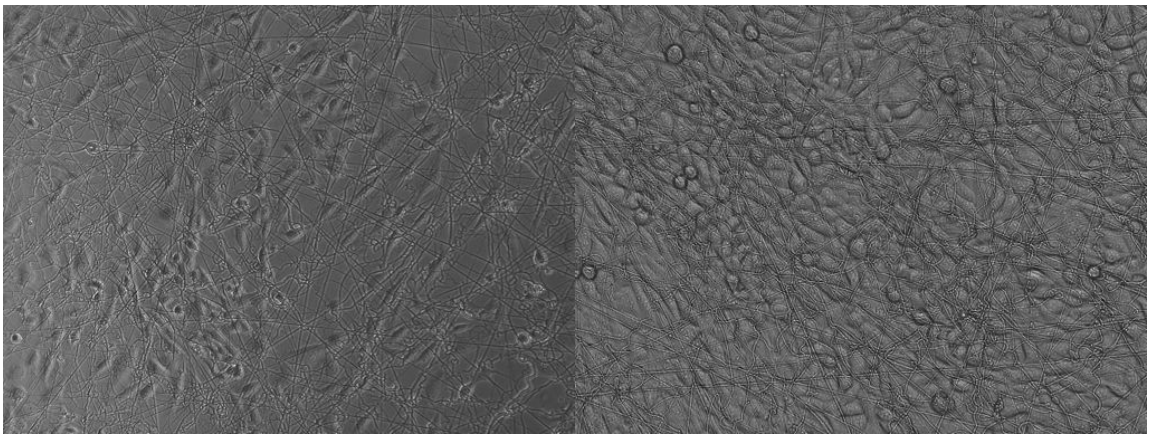

Figure 0.27: PCL nanofibers under a Type B film architecture. Brightfield images showing samples after 2 days (left, 10x magnification) and after 4 days (right, 20x magnification). Cell stretching, spreading, and proliferation were excellent. No fluorescence data shown, no GFP expression.

density to 20,000 (10,000 less than previous) to accommodate increased proliferation. We anticipated high transfection, and only MC3T3 cells were used. Duplicate films were fabricated in order to collect a greater breadth of data. In order to ensure the stability of the films after fabrication, they were UV sterilized instead of ethanol sterilized before use. Films received a top layer of fibronectin and briefly dried before being soaked in medium in sterile conditions to prime the sample for cell seeding. The medium was removed and the cells were seeded. As shown in figure 0.27, the cells not only attached but spread and stretched extremely well even by day 2. Proliferation and stretching was so high, that after 4 days the cells were confluent, even though seeding density had been reduced. Unfortunately, the great health of the cells did not ensure transfection, and through the 10 day experiment, no GFP expression was found in either sample.

Polyplex polycation testing and PEI toxicity

In order to evaluate transfection efficiency for 4 different polycations for using in the films, we ran a large polyplex transfection experiment. HEK-293, MC3T3, and NIH/3T3 cell lines were all used and the samples were performed in triplicate. The four polymers chosen were a newly synthesized linear PAA (AEPZ+APOL), PEI, RHB, and PolyJet as a positive control.

Modestly positive results for HEK-293 cells occurred with both PAA (figure 0.28)and RHB (figure0.29), unsurprising, as it this cell line has been reaffirmed as the easier of the 3 lines to transfect. The GFP expression for these two polymers however is somewhat muted in comparison to the PEI and PolyJet expression, and the number of cells transfected is much lower, as well. For

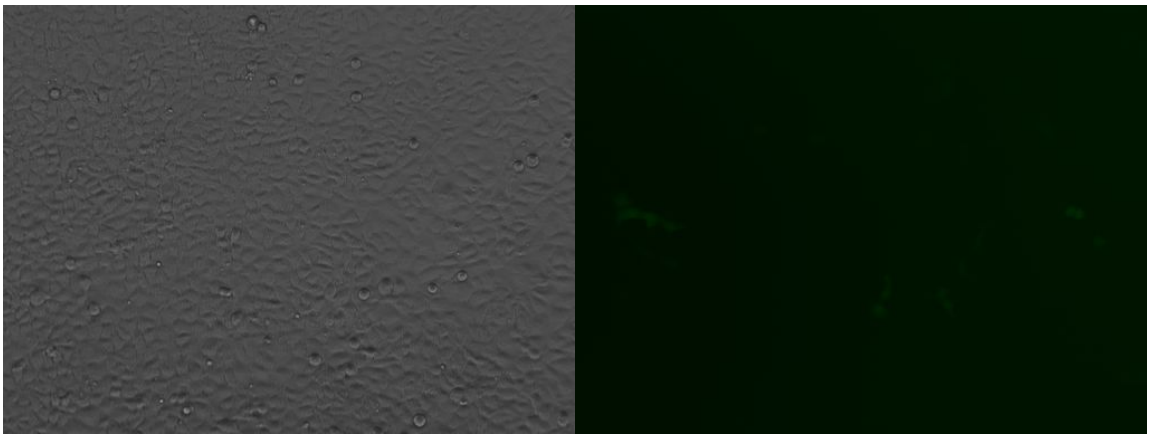

Figure 0.28: Polyplex results for newly synthesized PAA. Cell health is good, for all 3 cell lines (left, brightfield, HEK-293), although HEK-293 was the only cell line which showed GFP expression (right). 10x magnification.

PolyJet, PAA, and RHB, cell health is good for all 3 cell lines. In contrast, we found PEI to be relatively toxic at the concentration used (10/1 (w/w) ratio for polyplex formation). Surprisingly, cells were not killed off entirely, and so we are still able to see some transfection from both the HEK-293 and NIH/3T3 cell lines (figure 0.30). Future experiments will focus on optimizing PEI concentration in order to achieve transfection without the toxic side effects.

Widespread GFP expression (figure 0.31) shows reliable transfection for the PolyJet, and confirms the potency of the current batch of GFP-DNA. Even though all cell lines display widespread transfection with the PolyJet, it is interesting to point out the stark contrast between the GFP brightness between the 3 cell lines for PolyJet (again, figure 0.31). The dimness of the NIH/3T3, and especially the MC3T3 suggests that positive transfection results for these cell lines may be much more difficult to discern in fluorescence microscopy, and moving forward, should be evaluated differently than the HEK-293 cell line, and others that express GFP so vividly.

Introduction of p(APOL) and "thick film" architecture

A new polycation including 5-amino-1-pentanol (APOL) and new architecture were tested to try to improve transfection. Only HEK-293 cells used, and seeding density was reduced again to 15,000 cells(5,000 less than previous). The PAA synthesized was very complex, CBA+[AEPZ+APOL 1:1 n/n] (2:1 n/n), 50% labeled w/FITC. Hyaluronic acid was used as an intermittent polyanion, as shown in figure (0.32). Because of this arrangement, the number of film layers had to be increased in order to load the same amount of DNA as our normal Type B films. Instead of 16.5 bilayers, these films had 24.5 bilayers. Two films were fabricated, one having its terminal layer

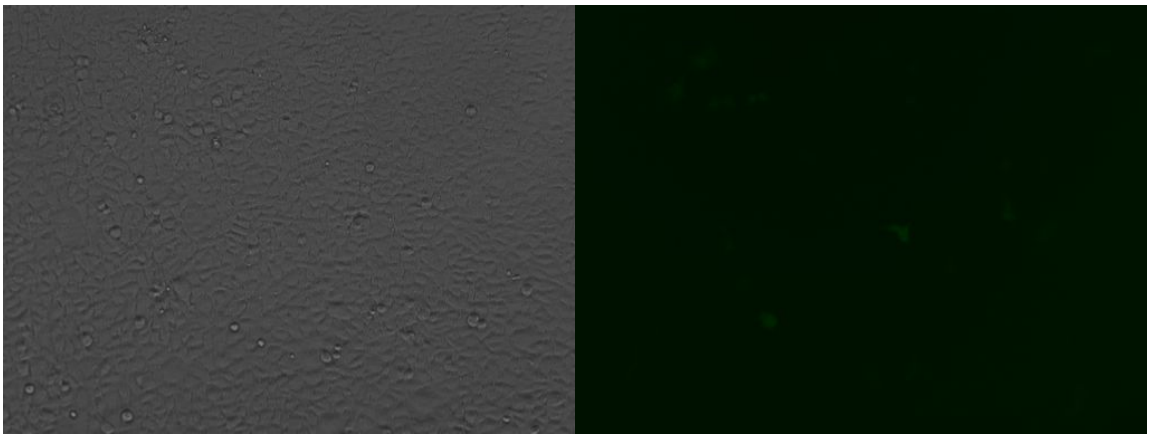

Figure 0.29: Polyplex results for RHB. Cell health is good, for all 3 cell lines (left, brightfield, HEK-293), although HEK-293 was the only cell line which showed GFP expression (right). 10x magnification.

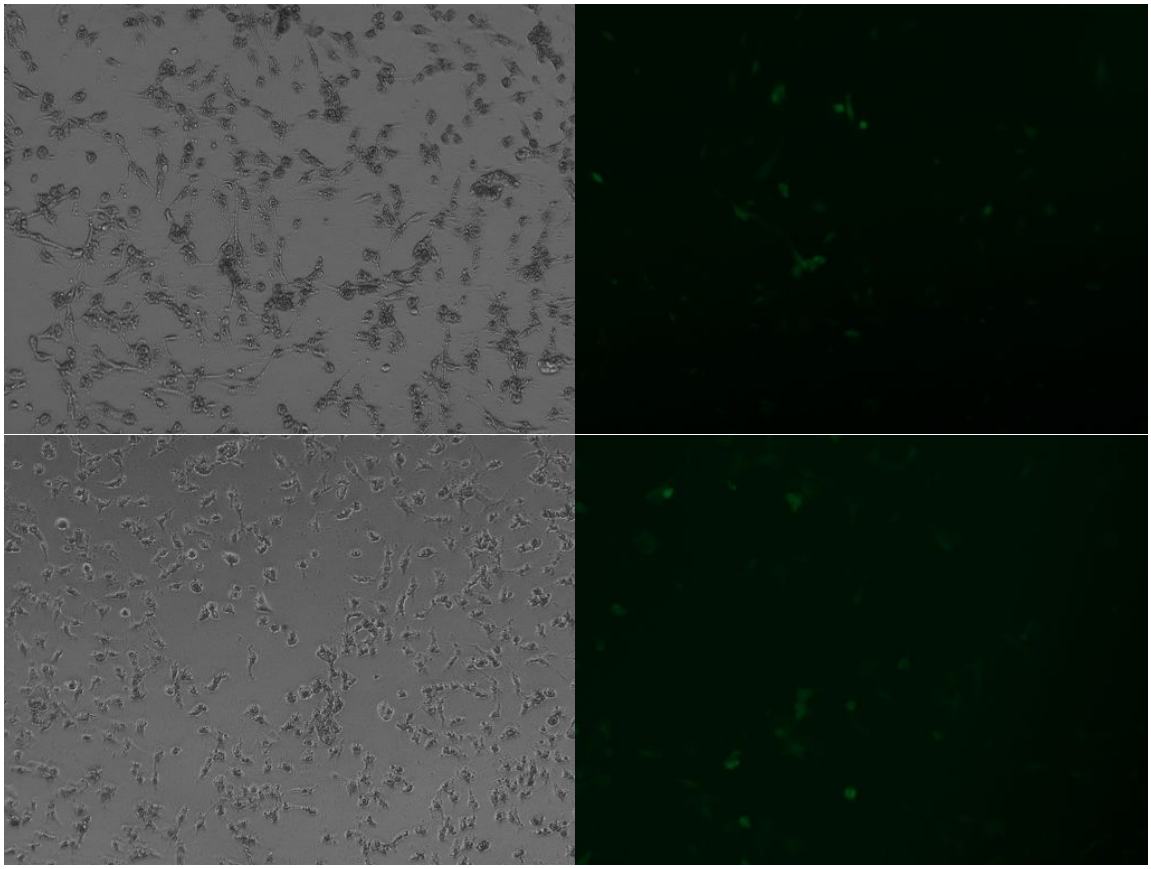

Figure 0.30: Polyplex results for PEI. Cell health is poor for all 3 cell lines, although NIH/3T3 cells (top) and HEK-293 cells (bottom) showed GFP expression despite visible toxicity. Left brightfield, right fluorescence. 10x magnification.

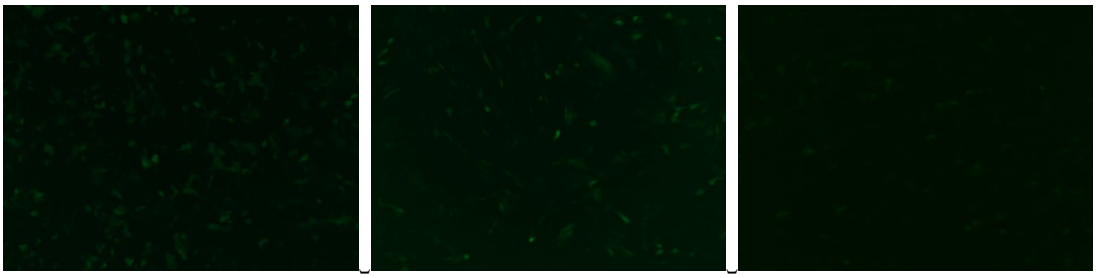

Figure 0.31: Polyplex results for PolyJet. Widespread GFP expression shows reliable transfection, and confirmation as a positive control. Cell health is good, for all 3 cell lines. HEK-293 (left) NIH/3T3 (center) and MC3T3 (right). Fluorescence, 10x magnification.

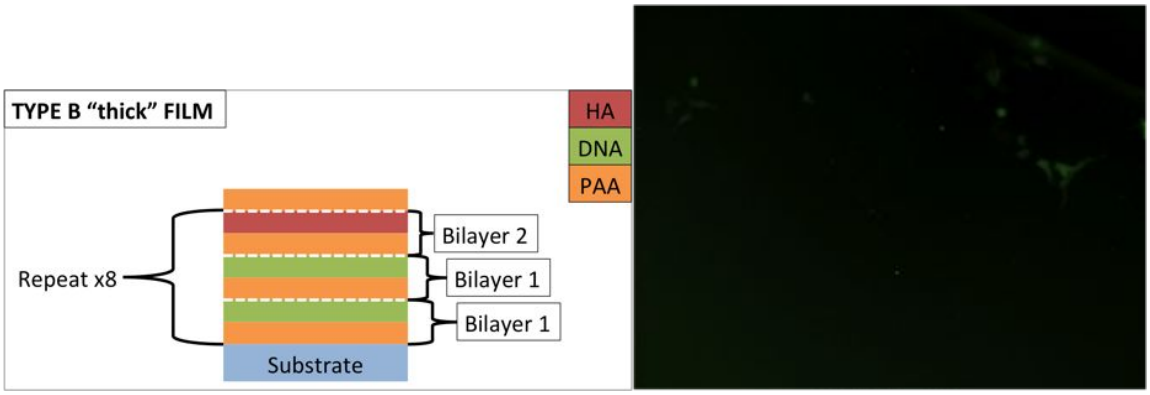

Figure 0.32: "Thick film" loads equivalent amount of DNA in 24.5 bilayers instead of traditional 16.5 bilayers, while substituting a second polyanion (HA) into the repeating pattern (left). Right: Cross-linked APOL/HA "thick film" at day 6, showing peak fluorescence of HEK-293. 10x magnification.

chemically cross-linked and one without cross-linking. Both films were terminated with a fibronectin layer. In contrast to the non-cross-linked sample, the cross-linked film showed GFP expression, and fluorescence peaked at 6 days (figure 0.32), dimming significantly at 8 days. It is important to note, that since these are the HEK-293 cells, this transfection can be categorized as minimal, as GFP expression was dim, and only occurred in isolated areas. Still, the polycation APOL is of interest, and will be investigated further.

Testing pAPOL transfection using polyplex

In order to further test the efficacy of the pAPOL used in the previous in vitro experiment, a polyplex experiment was set up using cell lines MC3T3, and NIH/3T3, which had not been used previously with the polymer. Two samples types (PAA polyplex and pAPOL polyplex) were tested in triplicate for each cell line. Briefly, the PAA was the same formulation as used in the previous experiment, (AEPZ+APOL). For the PAA polyplex samples, GFP expression was quite dim and

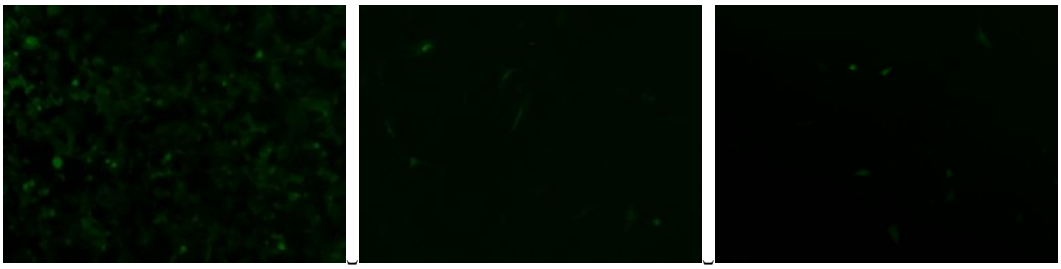

(a) Fluorescence images for pAPOL polyplex for each each cell line. High GFP expression shown in HEK-293 sample (left), medium GFP expression shown for MC3T3 (center) and low GFP expression shown for NIH/3T3 (right).

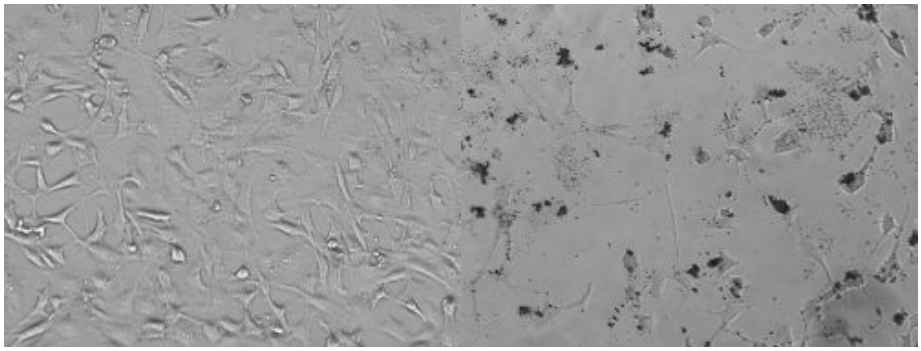

(b) Brightfield images showing possible pAPOL toxicity for the NIH/3T3 cell line. Other cell lines were unaffected. Part of the sample showing normal cell morphology (left) and an area of dark "granules", possibly toxicity, dead cell debris (right). Each of the 3 samples contained isolated areas with this abnormal morphology. Original images 10x magnification, zoomed in to show detail.

Figure 0.33: Polyplex experiment testing with pAPOL

not many cells transfected for any of the cell lines (data not shown). The pAPOL however did show a high degree of transfection, comparable to PolyJet for HEK-293 and MC3T3 (figure 0.33), and about half as much with the NIH/3T3 cell line. Additionally, the brightness of the GFP expression for the pAPOL MC3T3 is nearly identical to the PolyJet (0.31), which is very promising. Interestingly, there were signs of isolated toxicity in only the NIH/3T3 cell line for only the pAPOL samples. Features that we termed "granules" because of their granulated appearance, occurred in small areas in each of the 3 triplicate samples for the NIH/3T3 cell line (figure 0.33). Good transfection for MC3T3 and HEK-293, taken together with the isolated toxicity areas, the pAPOL results prompted further investigation into the polymer/DNA polyplex ratio and transfection capabilities of this polymer.

Large-scale p(APOL), p(APOL+MBA), and PEI polyplex ratio transfection testing

In order to explore the transfection efficiency between varying ratios of polymer-to-DNA for two batches of the same composition pAPOL, one batch of p(APOL+MBA), and PEI. pAPOL and

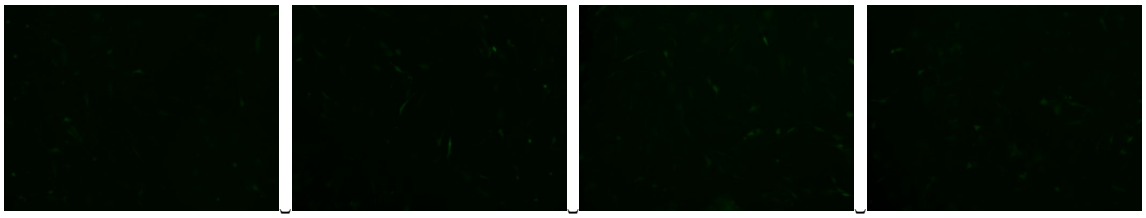

Figure 0.34: MC 3T3 cells showing GFP expression through various polyplexes, PolyJet (far left), pAPOL:DNA 75:1 (center left), pAPOL:DNA 1:100 (center right) and pAPOL:DNA 1:150 (far right). Although the fluorescence is dim, the GFP expression is substantial for this cell line, since PolyJet is a standard positive control. 10x magnification.

p(APOL+MBA) were both tested at ratios 25:1, 50:1, 75:1, and 100:1 and 150:1. PEI was tested at ratios 2.5:1 and 10:1, with 10:1 being the ratio used in all previous experiments. Surprisingly, the best results were batch A of pAPOL across the board for the HEK-293 samples, although batch B of pAPOL2 was the same composition as batch A, so there is clearly some inter-batch variability. With the PEI, there is toxicity seen in all cell lines for the 10:1 ratio, which was expected, and about half of the cells look visibly distressed, dehydrated, while there are scattered regions of cells that look perfectly healthy, and moderate-to-good GFP expression. Surprisingly, there was little to no toxicity for the 2.5:1 ratio of PEI, and also greater GFP expression for this ratio than the 10:1 ratio. Interestingly, for the PEI, the most transfection is seen in the PEI:DNA 2.5:1 ratio. There was no transfection for the p(APOL+MBA). Although dim, pAPOL batch A GFP expression was quite widespread for all of all 3 cell lines. Especially for MC3T3 (figure 0.34), the pAPOL batch A results are comparable or better than the PolyJet results, which is very promising for further polyplex experiments and also films. Unfortunately, without quantitative methods, it is unclear what ratio of pAPOL:DNA yields the brightest/most widespread GFP transfection. The brightfield images for the pAPOL and p(APOL+MBA) all look healthy, and even at high concentrations, there was no visible toxicity for the pAPOL. For PEI, the visual toxicity increases with increasing concentration. In addition to the different ratios of polycation:DNA, the cells were treated with comparable concentrations of just the polymer without any DNA. It was easy to see that even without polyplex formation caused from DNA, the PEI samples suffered toxicity issues, confirming that the PEI is at fault and not the PEI/DNA complex.

More polyplex testing with MBA, pAPOL, and PEI

This experiment focuses on MBA-pAPOL-DNA polyplexes. We tried a 50:1 ratio of p(APOL+MBA):DNA previously with no results from either cell line. The MBA replaces the CBA in the normal pAPOL structure. This experiment explores ratios from 25:1, 50:1, 75:1, and 100:1. Although the cells

look perfectly healthy, there was no transfection whatsoever for any of the MBA-pAPOL samples. There was transfection in both positive controls [PEI:DNA 2.5:1 (25 μl) and pAPOL:DNA 75:1 (50 μl)], so we know that the batch of DNA used was active. The results were approximately the same as the previous experiment for the two positive controls (PEI, pAPOL), thus confirming the data. This further enforces that pAPOL and PEI can achieve similar transfection results for the cell lines used here.

UV versus ethanol sterilization of thin film substrates before cell seeding

The effects of UV sterilization vs. ethanol sterilization are examined in order to open up possibilities to use less stabile molecules in our thin films that may be susceptible to degradation in ethanol. The films were kept simple, in fact, just a repeat experiment in order to get some better images and conclusive evidence Type A and Type B films. Since it was a repeat of previous work, variables were reverted to the previous work. Cell density had to be kept high, at 40,000 cells. Overcrowding and cell death precluded successful flow cytometry data, although cells from both UV and ethanol sterilization were effected, thus it seems that there was no appreciable difference in UV or ethanol sterilization methods.

MTT assay to determine cell viability. Polyplex testing with various polymers

18 samples for two cell lines, HEK-293 and MC3T3, were prepared for polyplex testing. In order to get an average, samples were run in triplicate for each of the polymers tested. Along with the pAPOL which yielded positive transfection results previously, a 33% CBA- and 67% CBA-PAA were tested at a polymer:DNA ratio of 1:50. These percentages coordinate to pAPOL with MBA:CBA ratio of 2:1 and 1:2, respectively. Along with these two CBA-containing polymers, PEI and pAPOL were tested, as positive controls. The results showed the HEK-293 cells being transfected comparably for the PEI and the pAPOL samples, with no transfection for either of the samples that contained CBA. The CBA samples did, however seem to be slightly toxic, as at least 1 sample from each 33% and 67% and also across both cell lines showed a shrunken, misshapen morphology. Of interest, there was strange morphology for some of the control samples of the MC3T3 cells. There was no reason to account for this, and perhaps the morphology was affected by something other than the polymer reaction, and had something to do with environmental changes, or the treatment of the cells (too much time washing, or drying in between applying various solutions

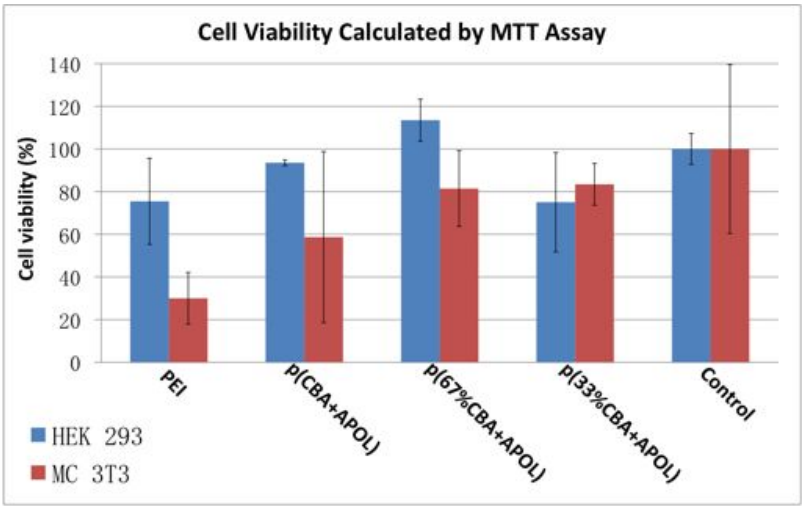

Figure 0.35: MTT assay results. A number of values were not included in the data show due to outlier activity. The trends within the cell lines and between the cell lines both differ.

during the procedure).

MTT results showed several things: first, there were several outliers (excluded from the data shown, figure 0.35). The first outlier excluded was for HEK-293. The PEI sample showed overwhelmingly positive GFP expression results for samples 1 and 2 (as expected), but with zero transfection for the third sample. As PEI has been shown many times before to be an efficient gene transfer polymer, this result was puzzling and pointed to human error, possibly to omission of the polyplex solution in this single sample out of a triplicate. Therefore, this data has not been included in the cell viability results, as they would skew the data to reflect a more viable population of cells similar to those of the untreated, very healthy control group rather than the cells treated with polyplex solutions, all of which have been shown to have various degrees of cytotoxicity. Additionally, the samples were done in triplicate and each of the triplicate samples was split into two samples because of the quantity required for the MTT assay, thus giving a total of 6 data points for each polyplex type. These data suggest different trends for the two cell lines. First, for the HEK-293 cells, the trend showed lowest cell viability for 33%CBA pAPOL and PEI (75.05% and 75.47% viability, respectively). Viability increased with pAPOL (93.55% viability), then the untreated control cells (used as baseline, "100% viability") and finally the 67% CBA pAPOL showed 113.52% viability. The oddness of this result can be explained by the vast number of variables introduced throughout the polyplex and MTT assay protocols. The seeding and cell preparation process for this procedure last several days, and the cells are still in the exponential growth phase. Coupled with errors in cell counting, cell dilution, and cell plating, it is easy to see how large amounts of

variation could be inevitably introduced in many steps throughout this particular process, and the sensitivity is high for the MTT assay, which may compound errors as well.

10.5 bilayer films with pAPOL, chitosan, and HA

MC3T3 cells were gown on a special 10.5 bilayer film including chitosan. Chitosan should help with attachment and spreading, thus facilitating transfection due to a more intimate connection and better interaction with the cells' extracellular environment. 10.5 bilayer samples with the pAPOL layers and HA/chitosan blend layers were fabricated in triplicate. The chitosan blend samples were each 10.5 bilayers, with pAPOL (4 bilayers total) being alternated with DNA (5 bilayers total) HA/chitosan (1.5 bilayers total), the pattern being similar in alternation of layers found with the "thick film" previously shown in figure 0.32. For sterilization of the film, UV only was used, as it was evidenced from previous experiments that there was no obvious difference between the two methods, and UV ensured that the new structure and components would not be exposed to ethanol. The cell seeding density was kept at 15,000 cells. Unfortunately, even though there was great attachment and proliferation, there was no GFP expression in any of the 10.5 bilayer special films with pAPOL and HA/chitosan.

Simple Type B pAPOL film transfection

pAPOL was very promising from our polyplex experiments, although the previous experiment showed no transfection, it was using a chitosan/HA blend, and the construction proved to be slightly different due to its constituents. Here, a normal Type B film with the pAPOL was made, coated with fibronectin, and compared to Type A film over 12 days. For positive controls, 25,000 kDa PEI polyplex and PolyJet polyplex samples were used and were prepared at the end of the 10 days. As is shown in figure 0.36, there is good GFP expression for the HEK-293 cells for the pAPOL. The two polyplex control samples, PEI and PolyJet, are shown for comparison only, since these are polyplex data and not LbL film data they cannot be directly compared for transfection efficiency.

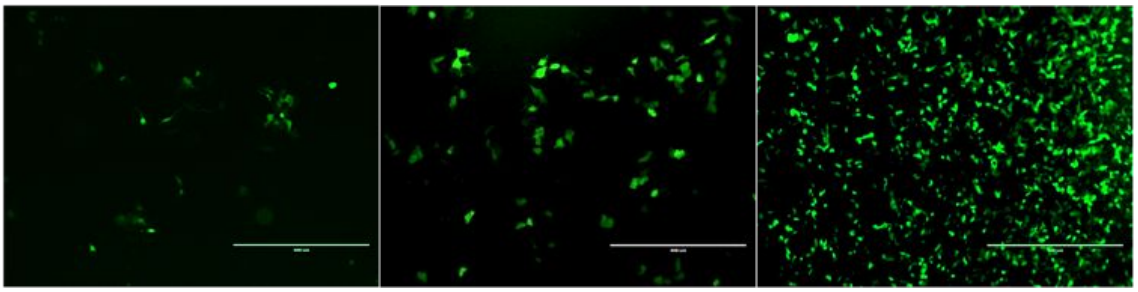

Figure 0.36: Day 12 images taken before flow cytometry. L-R: pAPOL Type B film, PEI polyplex positive control, PolyJet polyfection positive control. All HEK-293 cells, 10x magnification.

CHAPTER 4 DISCUSSION

This work provided insight on how a number of factors influence the efficacy of transfection on MC3T3, NIH/3T3 and HEK-293 cells. It lays the groundwork for further detailed studies optimizing polyelectrolyte components to achieve maximum transfection efficiency while minimizing cellular toxicity. There were a range of variables explored in this work, including LbL architecture, LbL film constituents, polyplex polyelectrolyte concentrations, in vitro experiment specifications, and DNA fabrication parameters. Experience and knowledge was gained and a number of important considerations for the future direction of polyelectrolyte thin films for gene delivery were revealed through these experiments. Not to be overlooked, the experimental parameters were optimized, materials protocols were reworked, and the framework for more reliable in vitro transfection were established through these studies.

LbL architecture

Previous work with Type A and Type B film architectures displayed the stark differences in the buildup and degradation characteristics between these films. However, these differences proved to be most evident in the transfection efficacy of these two types of films. Early on, GFP expression in any film was so low, that it was difficult to qualitatively differentiate between what was effective and what was not. As the parameters were changed and a reliable positive control was found in PolyJet, the ability of the Type B films to transfect cells when Type A films only showed inconclusive expression, became obvious.

From previous work, the role of film growth pattern and interlayer diffusion on the different release profiles between the two film types is apparent. It has also been shown that the presence of PEI as a barrier layer has been very effective, although it is unclear the extent of its influence on the transfection and ultimate gene expression of the LbL system. Unfortunately, transfection is still effectively a black box operation. There are a number of endocytic pathways and also a number of polyplex unpackaging theories, as well as different cytosolic transport mechanisms, and finally varied ways that the DNA gains nuclear import for expression. However, the scope of this project was not to gain understanding of the exceedingly intricate cellular pathways that the LbL film system employs. Instead, a broader knowledge of the system as a whole and the optimization of the complex components of the system itself were gained.

One concept that was tried and tested and held true throughout was that PEI is both an effective barrier layer, and an essential component of in order to achieve gene expression in our current system. Knowledge of PEI's toxicity was also acknowledged previously (reference [34], for example), but through polyplex assays, we were able to gain a better understanding of its working experimental limits as a potential toxic component The polyplex assays also helped realize the relationship between PEI concentration and gene expression. Within the Type B films structure classification, we also tested a thick film that was 24.5 bilayers instead of 16.5 bilayers. This film contained HA as an alternating polyanion layer, and so more layers were needed to incorporate a similar dose of DNA. Other than low transfection efficiency, we found no other side effects from this thicker structure, opening the possibility in the future for thicker films incorporating even more active molecules to cells.

LbL film constituents

Numerous polymers were tested as the non-PEI polycation layers in the Type B films to try to increase transfection efficiency. Our focus has always been on the disulfide bond-containing bioreducible PAAs, and within this category, we explored both the structure and the chemical makeup of these materials. For structure, we used either linear- or hyperbranched- (referred to previously as RHB) disulfide-containing cystamine bisacrylamide PAAs. Figure 0.7 shows the general chemical construction of these two structures of PAA, with linear being defined as a 1:1 ratio of bisacrylamide:AEPZ while RHB having a 2:1 ratio of bisacrylamide:AEPZ. Within the bisacrylamide portion, the ratio of cystamine- to methylamine- bisacrylamide can also be altered, allowing yet another degree of flexibility of the film on the molecular level.

After experimenting with different degrees of CBA content in both linear and RHB PAAs and only having mild GFP expression, we began testing with a new polymer, APOL. The blend that we used for the films was a 2:1 ratio of CBA to a 1/1 n/n ratio of APOL and AEPZ. Thus, it created a RHB with a lower AEPZ content. This new PAA turned out to aid in transfection for our system, and we had mild results when it was used in the new one-off "thick" film structure with HA using the HEK-293 cells, which are easiest to transfect in our experimental setup. We then used the APOL in polyplex experiments and found remarkable gene expression, similar to the positive control (PolyJet), even for the extremely difficult-to-transfect MC3T3 cell line. After polyplex experiments showed positive results, films were constructed that incorporated both APOL and the polysaccharide chitosan. Chitosan was chosen for its many features including biodegradability,

bioactivity, promotion of cell adhesion and growth, particularly in osteoblasts, as well as stimulation of osteogenesis and osteoblast differentiation [49, 50]. Chitosan is especially attractive for the MC3T3 preosteoblast cell line, which has proven to be the most difficult to achieve widespread and bright GFP expression in our LbL system.

These films were only 10.5 bilayers and followed a slightly altered Type B architecture in order to accommodate the chitosan, which was mixed with HA before film fabrication. Cell attachment, spreading and health were all excellent, and cells grew well enough that they started to look overcrowded quickly. There were no signs of cytotoxicity (only HEK-293 and MC3T3 cell lines were used. Previous toxicity issues with APOL and NIH/3T3 cell line). Unfortunately, we did not see the gene expression that we had seen for the polyplex experiments featuring APOL, and in fact there was no gene expression throughout the entire experiment. We hypothesize that the arrangement and concentrations of the components (chitosan, PEI, APOL, HA) can be reorganized in order for the system to achieve its full transfection potential.

Hyaluronic acid is a non-diffusible glucosaminoglycan found in extracellular matrix, among other bodily tissues. It is known to show bioactivity that is beneficial to our system, including antibacterial properties and involvement in cell migration, as well as generating compact nanoparticles when used alongside chitosan that have been shown to hold a high transfection efficiency [28, 51, 52]. There is also evidence that HA interacts strongly with PEI, which would result in facilitated uptake of polyplexes involving these two materials [14]. For these reasons, we used chitosan in conjunction with HA in our PEI-containing Type B films in hopes to increase the beneficial interactions between film surface and cell matrix and enhance transfection. However, it has also been shown that HA can be a cellular adhesion inhibitor as well [53]. Given our low transfection from our films, the HA concentration may need to be adjusted in order to balance its characteristics, as well as tuning the chitosan-HA interaction in order to realize their full cooperative benefits. A recent study showed the molecular weight of the chitosan involved in HA polyelectrolyte DNA delivery was an important factor in its transfection efficiency, with ultra-low molecular weights faring better [52].

The tripeptide sequence arginine-glycine-aspartic acid (RGD) is present on a number of extracellular matrix proteins including fibronectin, another component in our LbL films. When incorporated into a cellular substrate, such as our LbL films, it is known to directly mediate cell attachment [47], enhance cell adhesion and spreading [54]. Like chitosan, it is beneficial to have in our LbL system for all cell types, but in particular bone cells. A number of studies have shown various ways that RGD peptide can be an advantage to bone cell studies. One group found RGD biodegradable scaffolds promoted human osteoprogenitor differentiation [55], while another found a relationship

between surface density of RGD and enhanced osteoblast differentiation [56]. Yet another group used a combination of HA/chitosan/ RGD and found mammalian bone cell attachment, proliferation and function was enhanced [51], while also confirming their results with earlier work that showed a chitosan/RGD combination helped osteoblast migration, attachment, proliferation, and even mineralization [57].

Indeed, the addition of RGD enhanced gene expression in our films, although not as profoundly as may have been anticipated. For our films, we conjugated RGD to PEI and then used it as the barrier layer in the Type B film structure. This enhanced gene expression that we observed could certainly be increased by increasing the peptide density, using it as a standalone layer, or using it in addition to chitosan and HA.

While studies have shown cytotoxicity for PEI, they have also confirmed its ability to transfect cells with high efficiency [34]. Clearly a balance of these positive and negative attributes needs to be met. In order to best incorporate PEI into our specific LbL system, we performed polyplex experiments using different concentrations of PEI. We gained knowledge about the concentration limit that induces visible cytotoxicity and also both how the ratio of PEI to DNA as well as how the amount of toxicity affects the gene expression in our system. We examined a variety of other PAAs and how their concentration affected the gene expression as well, in order to determine the minimum material needed for successful transfection. This information is important for future in vivo studies, as the system should be tuned in order to maximize transfection and minimize waste and possible systemic exposure to the components.

Determining ideal DNA fabrication parameters proved extremely beneficial. Initially, the lack of high yield from the DNA amplification and purification procedures was persistent. The variables that were tuned included bacterial growing time, culture preparation, and bacterial host. Using spectrophotometric data, performing agarose gels, and after many iterations, a reliable procedure was developed that increased our mg/mL yield nearly 4-fold from earlier versions.

In vitro experiment specifications

Another aspect of our LbL system that was evaluated and improved was the in vitro experimental setup. The way our LbL film system is implemented follows a careful approach that takes into consideration how the film and its surroundings would interact in the future in vivo setting. The film is coated onto a rigid substrate, placed in the bottom of a tissue culture well, and then the cells are allowed to engage the film surface to the degree of which the cells determine. Unlike other

methods of in vitro testing, where the film is forced into contact with an already established cell population, our method is more realistic and encourages engineering of the film surface to best suit the extracellular needs of the cells. In this way, we can not only determine if the film itself has good transfection capabilities, but determine if the system encourages cell growth, attachment, and other preliminary criteria for transfection. Since our films' mechanisms for biodegradation and DNA delivery rely on the interaction of the cells with the film, making sure the cells don't need to be forced unto the film for transfection is a critical design point.

In order to ensure both a hospitable and unbiased environment for the cells, we employ a number of key features. The first is that the bottom of the tissue culture wells are coated with poly(HEMA) which prevents cellular attachment and spreading. This ensures that the cells do not preferentially attach to the very accommodating tissue culture-treated bottom of the well. Coating the plates with poly(HEMA), although straightforward requires a bit of finesse in order to execute a smooth, even platform for the substrate to sit upon. Additionally, we discovered early on that in order to acquire the best results as far as both cell growth and microscopy, the substrate should be placed in the smallest-sized well possible, eliminating excess surface area and minimizing shifting and movement of the intricate setup. Sterilization of the substrate and the system was another aspect that was evaluated. UV was utilized for the culture plates while a series of ethanol baths and rinses was used for the substrates. However, as experiments progressed and more fragile components were being tested in the films, we started to asses if UV could also be used for the substrates. Although UV versus ethanol sterilization was not tested in depth, from preliminary experiments, they seemed comparable, if not indistinguishable.

Chemical cross-linking of the top bilayer (cell-interacting top surface of the film) proved to be a very important step in increasing both cell adhesion and transfection efficiency for our system. With certain polymers and architectures, cross-linking was the difference between gene expression and negative results. Initially, films were cross-linked on a single side. Unfortunately, due to the amount of transfer and handling of the substrates, having a right- and wrong- configuration quickly became a source of frustration. Moving forward, both sides were cross-linked, and in fact different cross-linking times were tested. Qualitatively, we found a slight increase in the number of cells that attached and grew on the substrates with longer cross-linking time.

Another variable that we determined was of high importance was the application of a fibronectin top layer to the film directly before seeding the cells on the substrate. Early on we established rough guidelines for the incubation time and concentration, which were further refined until a practical protocol was established. Finding an appropriate cell seeding density was another variable that took

careful consideration. The film components varied wildly from experiment to experiment, sometimes having a polymer with known positive bioactivity, and sometimes with a polymer that tended toward anti-attachment properties. Because of this variance, sometimes cells grew swifter than anticipated and were soon overgrown, precluding adequate results and causing early termination of the experiments. The differences in cell growth and behavior between cell lines also made pinpointing an ideal cell seeding density for each experimental setup precarious.

Future work

An abundance of knowledge was gathered through these experiences that provide keen insight into the future direction of this project. Now that experimental methods and procedures have been established and the groundwork has been laid, there are a number of ways to move forward. The vast number of variables involved in non-viral drug delivery systems made qualitative evaluations a first step. Our evaluation methods leave much room for understanding the mechanisms of both uptake and expression of genes in our LbL film-cellular environment systems. In order to gain more precise insight into the mechanisms of this intricate system, methods of quantitative evaluation should be explored. Flow cytometry could be an invaluable resource for these thin film systems, giving an exact count of successfully transfected cells showing GFP protein expression. Not only could the GFP expression be evaluated, but fluorophores could be used to fluorescently tag different elements of the polymeric compounds, shedding light onto how the internalization process is carried out on our film systems. This same concept could be used with confocal microscopy. The MTT assay was used as an indicator for cellular viability, but flow cytometry could also be used for this purpose, streamlining the characterization process for these transfected cells.

More in depth polymer characterization can be performed, pinpointing the best polymer chain architecture (branching, etc.), molecular weight, and other details that will allow more precise degradation tuning for the system. The relationship between the different constituents can be further explored, noting the intricate balance between concentrations and placement of RGD, HA, chitosan, and others. Moving forward, it would be sensible to run at least duplicate or triplicate samples in order to gain more evaluation power and understand intra-sample variability in this complex LbL system.

The broader scope of this system would look into testing LbL parameters for transfection of functional genes, not just the GFP reporter gene used here. Additionally, a wider variety of practical cell lines should be investigated. The orthopedic model would be an exemplary application for our

LbL thin film technology, where controlled release of multiple growth factors and signaling proteins is critical. Although PEI is an ideal barrier layer for our system, its toxicity potential may eventually become a hindrance. In the future, finding a more biologically neutral material for our barrier layer would certainly add to the marketability of our LbL delivery system.

By optimizing the experimental parameters and materials protocols for the complex system of testing our non-viral bioreducible polyelectrolyte LbL thin film DNA delivery system, the framework for more reliable in vitro transfection was established. This lays a foundation and opens up a great opportunity to build upon this knowledge and further the understanding and characterization of these very promising LbL films and their components.

REFERENCES

[1] M. M. De Villiers, D. P. Otto, S. J. Strydom, and Y. M. Lvov, "Introduction to nanocoatings produced by layer-by-layer (lbl) self-assembly," *Advanced drug delivery reviews*, vol. 63, no. 9, pp. 701–715, 2011.

[2] C. J. Lavernia, M. K. Drakeford, A. K. Tsao, A. Gittelsohn, K. A. Krackow, and D. S. Hungerford, "Revision and primary hip and knee arthroplasty: A cost analysis." *Clinical orthopaedics and related research*, vol. 311, pp. 136–141, 1995.

[3] A. J. Weiss, A. Elixhauser, and R. M. Andrews, "Characteristics of operating room procedures in us hospitals, 2011," 2014.

[4] S. Kurtz, K. Ong, E. Lau, F. Mowat, and M. Halpern, "Projections of primary and revision hip and knee arthroplasty in the united states from 2005 to 2030," *The Journal of Bone & Joint Surgery*, vol. 89, no. 4, pp. 780–785, 2007.

[5] A. Ince, J. Rupp, L. Frommelt, A. Katzer, J. Gille, and J. Löhr, "Is ÒaseptícÓ loosening of the prosthetic cup after total hip replacement due to nonculturable bacterial pathogens in patients with low-grade infection?" *Clinical infectious diseases*, vol. 39, no. 11, pp. 1599–1603, 2004.

[6] W. H. Harris and C. B. Sledge, "Total hip and total knee replacement," *New England Journal of Medicine*, vol. 323, no. 11, pp. 725–731, 1990.

[7] J. Street, M. Bao, S. Bunting, F. V. Peale, N. Ferrara, H. Steinmetz, J. Hoeffel, J. L. Cleland, A. Daugherty, N. van Bruggen *et al.*, "Vascular endothelial growth factor stimulates bone repair by promoting angiogenesis and bone turnover," *Proceedings of the National Academy of Sciences*, vol. 99, no. 15, pp. 9656–9661, 2002.

[8] N. J. Shah, M. L. Macdonald, Y. M. Beben, R. F. Padera, R. E. Samuel, and P. T. Hammond, "Tunable dual growth factor delivery from polyelectrolyte multilayer films," *Biomaterials*, vol. 32, no. 26, pp. 6183–6193, 2011.

[9] C. R. Bragdon, M. Jasty, M. Greene, H. E. Rubash, and W. H. Harris, "Biologic fixation of total hip implants," *The Journal of Bone & Joint Surgery*, vol. 86, no. suppl 2, pp. 105–117, 2004.

[10] P. T. Hammond, "Building biomedical materials layer-by-layer," *Materials Today*, vol. 15, no. 5, pp. 196–206, 2012.

[11] E. Leguen, A. Chassepot, G. Decher, P. Schaaf, J.-C. Voegel, and N. Jessel, "Bioactive coatings based on polyelectrolyte multilayer architectures functionalized by embedded proteins, peptides

or drugs," *Biomolecular engineering*, vol. 24, no. 1, pp. 33–41, 2007.

[12] M. L. Macdonald, R. E. Samuel, N. J. Shah, R. F. Padera, Y. M. Beben, and P. T. Hammond, "Tissue integration of growth factor-eluting layer-by-layer polyelectrolyte multilayer coated implants," *Biomaterials*, vol. 32, no. 5, pp. 1446–1453, 2011.

[13] S. C. Gangloff, G. Ladam, V. Dupray, K. Fukase, K. Brandenburg, M. Guenounou, P. Schaaf, J.-C. Voegel, and N. Jessel, "Biologically active lipid a antagonist embedded in a multilayered polyelectrolyte architecture," *Biomaterials*, vol. 27, no. 9, pp. 1771–1777, 2006.

[14] S. Y. Wong, J. M. Pelet, and D. Putnam, "Polymer systems for gene deliveryÑpast, present, and future," *Progress in Polymer Science*, vol. 32, no. 8, pp. 799–837, 2007.

[15] D. W. Pack, A. S. Hoffman, S. Pun, and P. S. Stayton, "Design and development of polymers for gene delivery," *Nature Reviews Drug Discovery*, vol. 4, no. 7, pp. 581–593, 2005.

[16] R. Pawliuk, K. A. Westerman, M. E. Fabry, E. Payen, R. Tighe, E. E. Bouhassira, S. A. Acharya, J. Ellis, I. M. London, C. J. Eaves *et al.*, "Correction of sickle cell disease in transgenic mouse models by gene therapy," *Science*, vol. 294, no. 5550, pp. 2368–2371, 2001.

[17] E. Burton, J. Glorioso, and D. Fink, "Gene therapy progress and prospects: Parkinson's disease," *Gene Therapy*, vol. 10, no. 20, pp. 1721–1727, 2003.

[18] J. C. Van Deutekom and G.-J. B. Van Ommen, "Advances in duchenne muscular dystrophy gene therapy," *Nature Reviews Genetics*, vol. 4, no. 10, pp. 774–783, 2003.

[19] S. Ferrari, D. M. Geddes, and E. W. Alton, "Barriers to and new approaches for gene therapy and gene delivery in cystic fibrosis," *Advanced drug delivery reviews*, vol. 54, no. 11, pp. 1373–1393, 2002.

[20] M. A. Kay, C. S. Manno, M. V. Ragni, P. J. Larson, L. B. Couto, A. McClelland, B. Glader, A. J. Chew, J. Shing, R. W. Herzog *et al.*, "Evidence for gene transfer and expression of factor ix in haemophilia b patients treated with an aav vector," *Nature genetics*, vol. 24, no. 3, pp. 257–261, 2000.

[21] R. Coleman, "Risks and benefits of bisphosphonates," *British journal of cancer*, vol. 98, no. 11, pp. 1736–1740, 2008.

[22] F. Daubiné, D. Cortial, G. Ladam, H. Atmani, Y. Haïkel, J.-C. Voegel, P. Clézardin, and N. Benkirane-Jessel, "Nanostructured polyelectrolyte multilayer drug delivery systems for bone metastasis prevention," *Biomaterials*, vol. 30, no. 31, pp. 6367–6373, 2009.

[23] M. Liu, "Dna vaccines: a review," *Journal of internal medicine*, vol. 253, no. 4, pp. 402–410, 2003.

[24] A. M. Krieg, "Lymphocyte activation by cpg dinucleotide motifs in prokaryotic dna," *Trends*

in microbiology, vol. 4, no. 2, pp. 73–77, 1996.

[25] Y. Sato, M. Roman, H. Tighe, D. Lee, M. Corr, M.-D. Nguyen, G. J. Silverman, M. Lotz, D. A. Carson, and E. Raz, "Immunostimulatory dna sequences necessary for effective intradermal gene immunization," *Science*, vol. 273, no. 5273, pp. 352–354, 1996.

[26] D. M. Klinman, G. Yamshchikov, and Y. Ishigatsubo, "Contribution of cpg motifs to the immunogenicity of dna vaccines." *The Journal of Immunology*, vol. 158, no. 8, pp. 3635–3639, 1997.

[27] R. P. Johnson, "Live attenuated aids vaccines: hazards and hopes," *Nature medicine*, vol. 5, no. 2, pp. 154–155, 1999.

[28] S. B. Goodman, Z. Yao, M. Keeney, and F. Yang, "The future of biologic coatings for orthopaedic implants," *Biomaterials*, vol. 34, no. 13, pp. 3174–3183, 2013.

[29] D. Schaffert and E. Wagner, "Gene therapy progress and prospects: synthetic polymer-based systems," *Gene therapy*, vol. 15, no. 16, pp. 1131–1138, 2008.

[30] C. M. Jewell and D. M. Lynn, "Multilayered polyelectrolyte assemblies as platforms for the delivery of dna and other nucleic acid-based therapeutics," *Advanced drug delivery reviews*, vol. 60, no. 9, pp. 979–999, 2008.

[31] C. Lin and J. F. Engbersen, "Effect of chemical functionalities in poly (amido amine) s for non-viral gene transfection," *Journal of Controlled Release*, vol. 132, no. 3, pp. 267–272, 2008.

[32] C. Lin, Z. Zhong, M. C. Lok, X. Jiang, W. E. Hennink, J. Feijen, and J. F. Engbersen, "Novel bioreducible poly (amido amine) s for highly efficient gene delivery," *Bioconjugate chemistry*, vol. 18, no. 1, pp. 138–145, 2007.

[33] S. Takae, K. Miyata, M. Oba, T. Ishii, N. Nishiyama, K. Itaka, Y. Yamasaki, H. Koyama, and K. Kataoka, "Peg-detachable polyplex micelles based on disulfide-linked block catiomers as bioresponsive nonviral gene vectors," *Journal of the American Chemical Society*, vol. 130, no. 18, pp. 6001–6009, 2008.

[34] L. Parhamifar, A. K. Larsen, A. C. Hunter, T. L. Andresen, and S. M. Moghimi, "Polycation cytotoxicity: a delicate matter for nucleic acid therapy–focus on polyethylenimine," *Soft Matter*, vol. 6, no. 17, pp. 4001–4009, 2010.

[35] K. von Gersdorff, N. N. Sanders, R. Vandenbroucke, S. C. De Smedt, E. Wagner, and M. Ogris, "The internalization route resulting in successful gene expression depends on both cell line and polyethylenimine polyplex type," *Molecular Therapy*, vol. 14, no. 5, pp. 745–753, 2006.

[36] S. K. Lai, K. Hida, C. Chen, and J. Hanes, "Characterization of the intracellular dynamics of a non-degradative pathway accessed by polymer nanoparticles," *Journal of Controlled Release*,

vol. 125, no. 2, pp. 107–111, 2008.

[37] J. Suh, D. Wirtz, and J. Hanes, "Efficient active transport of gene nanocarriers to the cell nucleus," *Proceedings of the National Academy of Sciences*, vol. 100, no. 7, pp. 3878–3882, 2003.

[38] S. Brunner, E. Fürtbauer, T. Sauer, M. Kursa, and E. Wagner, "Overcoming the nuclear barrier: cell cycle independent nonviral gene transfer with linear polyethylenimine or electroporation," *Molecular Therapy*, vol. 5, no. 1, pp. 80–86, 2002.

[39] S. Brunner, T. Sauer, S. Carotta, M. Cotten, M. Saltik, and E. Wagner, "Cell cycle dependence of gene transfer by lipoplex, polyplex and recombinant adenovirus," *Gene therapy*, vol. 7, no. 5, pp. 401–407, 2000.

[40] S. Grosse, G. Thévenot, M. Monsigny, and I. Fajac, "Which mechanism for nuclear import of plasmid dna complexed with polyethylenimine derivatives?" *The journal of gene medicine*, vol. 8, no. 7, pp. 845–851, 2006.

[41] D. V. Schaffer, N. A. Fidelman, N. Dan, and D. A. Lauffenburger, "Vector unpacking as a potential barrier for receptor-mediated polyplex gene delivery," *Biotechnology and bioengineering*, vol. 67, no. 5, pp. 598–606, 2000.

[42] V. A. Bloomfield *et al.*, "Dna condensation by multivalent cations," *Biopolymers*, vol. 44, no. 3, pp. 269–282, 1997.

[43] T. Scientific, "Assessment of nucleic acid purity," Thermo Scientific, Tech. Rep., January 2011.

[44] ——, "Interpretation of nucleic acid 260/280 ratios," Thermo Scientific, Tech. Rep., January 2012.

[45] P. Brescia, "Micro-volume purity assessment of nucleic acids using a260/a280 ratio and spectral scanning," BioTek Instruments, Winooski, VT, Tech. Rep. AN060112-12, Rev. 06-04-12, June 2012.

[46] Y. Zou, L. Xie, S. Carroll, M. Muniz, H. Gibson, W.-Z. Wei, H. Liu, and G. Mao, "Layer-by-layer films with bioreducible and nonbioreducible polycations for sequential dna release," *Biomacromolecules*, vol. 15, no. 11, pp. 3965–3975, 2014.

[47] E. Ruoslahti and M. D. Pierschbacher, "Arg-gly-asp: a versatile cell recognition signal," *Cell*, vol. 44, no. 4, pp. 517–518, 1986.

[48] W. Song, D. C. Markel, S. Wang, T. Shi, G. Mao, and W. Ren, "Electrospun polyvinyl alcohol–collagen–hydroxyapatite nanofibers: a biomimetic extracellular matrix for osteoblastic cells," *Nanotechnology*, vol. 23, no. 11, p. 115101, 2012.

[49] A. K. Gaharwar, P. J. Schexnailder, Q. Jin, C.-J. Wu, and G. Schmidt, "Addition of chitosan

to silicate cross-linked peo for tuning osteoblast cell adhesion and mineralization," *ACS applied materials & interfaces*, vol. 2, no. 11, pp. 3119–3127, 2010.

[50] J. Guzmán-Morales, H. El-Gabalawy, M. H. Pham, N. Tran-Khanh, M. D. McKee, W. Wu, M. Centola, and C. D. Hoemann, "Effect of chitosan particles and dexamethasone on human bone marrow stromal cell osteogenesis and angiogenic factor secretion," *Bone*, vol. 45, no. 4, pp. 617–626, 2009.

[51] P.-H. Chua, K.-G. Neoh, E.-T. Kang, and W. Wang, "Surface functionalization of titanium with hyaluronic acid/chitosan polyelectrolyte multilayers and rgd for promoting osteoblast functions and inhibiting bacterial adhesion," *Biomaterials*, vol. 29, no. 10, pp. 1412–1421, 2008.

[52] N. Duceppe and M. Tabrizian, "Factors influencing the transfection efficiency of ultra low molecular weight chitosan/hyaluronic acid nanoparticles," *Biomaterials*, vol. 30, no. 13, pp. 2625–2631, 2009.

[53] C. A. Holmes and M. Tabrizian, "Substrate-mediated gene delivery from glycol-chitosan/hyaluronic acid polyelectrolyte multilayer films," *ACS applied materials & interfaces*, vol. 5, no. 3, pp. 524–531, 2013.

[54] R. A. Quirk, W. C. Chan, M. C. Davies, S. J. Tendler, and K. M. Shakesheff, "Poly (l-lysine)–grgds as a biomimetic surface modifier for poly (lactic acid)," *Biomaterials*, vol. 22, no. 8, pp. 865–872, 2001.

[55] X. Yang, H. Roach, N. Clarke, S. Howdle, R. Quirk, K. Shakesheff, and R. Oreffo, "Human osteoprogenitor growth and differentiation on synthetic biodegradable structures after surface modification," *Bone*, vol. 29, no. 6, pp. 523–531, 2001.

[56] A. Rezania and K. E. Healy, "The effect of peptide surface density on mineralization of a matrix deposited by osteogenic cells," *Journal of biomedical materials research*, vol. 52, no. 4, pp. 595–600, 2000.

[57] J. Li, H. Yun, Y. Gong, N. Zhao, and X. Zhang, "Investigation of mc3t3-e1 cell behavior on the surface of grgds-coupled chitosan," *Biomacromolecules*, vol. 7, no. 4, pp. 1112–1123, 2006.

ABSTRACT

PROGRAMMABLE DNA DELIVERY TO CELLS USING BIOREDUCIBLE LAYER-BY-LAYER (LBL) POLYELECTROLYTE THIN FILMS

by

MARIA MUÑIZ

May 2015

Advisor: Dr. Guangzhao Mao

Major: Biomedical Engineering

Degree: Master of Science

Bioreducible, layer-by-layer (LbL) polyelectrolyte films show great promise for use in biomedical implant and gene-delivery applications. These nanometer-scale thin films can easily be coated onto a variety of implantable surfaces or devices. To achieve proof of concept, HEK-293, NIH/3T3, RAW, and MC3T3 cells were transfected using plasmid DNA with the green fluorescent protein reporter gene (GFP-DNA). In order to optimize transfection, a number of polyelectrolytes and biological components were systematically incorporated into the two similar basic LbL structures. Based on our previous degradation assays, it is shown that cellular interactions in vitro can break down the layers of the thin films on substrates, allowing for DNA and future therapeutics to be released gradually over periods of time, or in bulk, depending on modifications to the structure and composition. Using an efficient in vitro polyplex testing method, different bioreducible polycations were examined in order to select a polyelectrolyte with high transfection. Following polyplex testing, thin films were made using the layer-by-layer dip coating method and cells were cultured on the subsequent films in an in vitro setting. The basic LbL structure comprises alternating polycation, GFP-DNA, and polyethylenimine (PEI) as an effective barrier layer. In vitro testing for transfection was monitored using fluorescence microscopy over 10 days, among other evaluation methods. Through these studies, transfection was achieved. This lays the groundwork for future studies using bioreducible thin films to deliver DNA, small molecules, or other therapeutics to cells.

AUTOBIOGRAPHICAL STATEMENT

MARIA MUÑIZ

EDUCATION

- B.S.E., Materials Science & Engineering, University of Michigan, Ann Arbor, MI (2009)

EXPERIENCE

- 06/2014 - 08/2014, Richard Barber Interdisciplinary Summer Research Program, Wayne State University, Detroit, MI
- 10/2009 - 01/2013, Hematology Oncology Research Technician Intermediate, University of Michigan Comprehensive Cancer Center, Ann Arbor, MI

PUBLICATIONS

1. Paoletti, C., Li, Y., **Muniz, M. C.**, Kidwell, K. M., Aung, K., Thomas, D. G., ... & Hayes, D. F. (2015). Significance of Circulating Tumor Cells in metastatic triple negative breast cancer patients within a randomized, phase II trial: TBCRC 019. Clinical Cancer Research, clincanres-2781.
2. Zou, Y., Xie, L., Carroll, S., **Muniz, M.**, Gibson, H., Wei, W. Z., ... & Mao, G. (2014). Layer-by-Layer Films with Bioreducible and Nonbioreducible Polycations for Sequential DNA Release. Biomacromolecules, 15(11), 3965-3975.
3. Paoletti, C., **Muniz, M. C.**, Thomas, D. G., Griffith, K. A., Kidwell, K. M., Tokudome, N., ... & Hayes, D. F. (2014). Development of Circulating Tumor Cell-Endocrine Therapy Index in Patients with Hormone Receptor Positive Breast Cancer. Clinical Cancer Research, clincanres-1913.
4. Smerage, J. B., Budd, G. T., Doyle, G. V., Brown, M., Paoletti, C., **Muniz, M.**, ... & Hayes, D. F. (2013). Monitoring apoptosis and Bcl-2 on circulating tumor cells in patients with metastatic breast cancer. Molecular oncology, 7(3), 680-692.
5. Shukla, R., Hill, E., Shi, X., Kim, J., **Muniz, M. C.**, Sun, K., & Baker, J. R. (2008). Tumor microvasculature targeting with dendrimer-entrapped gold nanoparticles. Soft Matter, 4(11), 2160-2163.
6. Shi, X., Lesniak, W., Islam, M. T., **Muñiz, M. C.**, Balogh, L. P., & Baker, J. R. (2006). Comprehensive characterization of surface-functionalized poly (amidoamine) dendrimers with acetamide, hydroxyl, and carboxyl groups. Colloids and Surfaces A: Physicochemical and Engineering Aspects, 272(1), 139-150.